This is the accepted manuscript published as Zeng, B., Yuan, C., Yang, X., L. Atkin, S., & Xu, S. (2013). TRPC Channels and Their Splice Variants are Essential for Promoting Human Ovarian Cancer Cell Proliferation and Tumorigenesis. *Current Cancer Drug Targets*, 13(1), 103-116. https://doi.org/10.2174/156800913804486629

TRPC Channels and Their Splice Variants are Essential for Promoting Human Ovarian Cancer Cell Proliferation and Tumorigenesis

Running title: TRPC Channels in Ovarian Cancer

Bo Zeng[1], Cunzhong Yuan[2], Xingsheng Yang[2], Stephen L. Atkin[1], Shang-Zhong Xu[1*]

[1]Diabetes, Endocrinology and Metabolism, Hull York Medical School, University of Hull, Hull, UK

[2]Department of Obstetrics and Gynaecology, Qilu Hospital of Shandong University, Jinan 250012, China.

[*]Correspondence:

Dr. Shang-Zhong Xu
Department of Diabetes, Endocrinology and Metabolism, Hull York Medical School
University of Hull, Cottingham Road, Hull, HU6 7RX, United Kingdom
Tel: +44 1482 465372, Fax: +44 1482 465390, e-mail: sam.xu@hyms.ac.uk

Footnotes. GenBank accession number for TRPC1 spliced isoform: GQ293239**.**

Abstract: TRPC channels are Ca^{2+}-permeable cationic channels controlling Ca^{2+} influx response to the activation of G protein-coupled receptors and protein tyrosine kinase pathways or the depletion of Ca^{2+} stores. Here we aimed to investigate whether TRPC can act as the potential therapeutic targets for ovarian cancer. The mRNAs of TRPC1, TRPC3, TRPC4 and TRPC6 were detected in human ovarian adenocarcinoma. The spliced variants of TRPC1β, TRPC3a, TRPC4β, TRPC4γ, and TRPC6 with exon 3 and 4 deletion were highly expressed in the ovarian cancer cells, and a novel spliced isoform of TRPC1 with exon 9 deletion ($TRPC1^{E9del}$) was identified. TRPC proteins were also detected by Western blotting and immunostaining. The expression of TRPC1, TRPC3, TRPC4 and TRPC6 was significantly lower in the undifferentiated ovarian cancer cells, but all-*trans* retinoic acid up-regulated the gene expression of TRPCs. The expression level was correlated to the cancer differentiation grade. The non-selective TRPC channel blockers, 2-APB and SKF-96365, significantly inhibited the cell proliferation, whilst the increase of TRPC channel activity by trypsin promoted the cell proliferation. Transfection with siRNA targeting TRPC1, TRPC3, TRPC4 and TRPC6 or application of specific blocking antibodies targeting to TRPC channels inhibited the cell proliferation. On the contrary, overexpression of TRPC1, $TRPC1^{E9del}$, TRPC3, TRPC4, and TRPC6 increased the cancer cell colony growth. These results suggest that TRPCs and their spliced variants are important for human ovarian cancer development and alternation of the expression or activity of these channels could be a new strategy for anticancer therapy.

Keywords: calcium channels, ovarian cancer, proliferation, SKOV3 cells, TRPC

INTRODUCTION

Ca^{2+} is a second messenger which plays a major role in the regulation of cellular functions, such as contraction, secretion, cell growth and death. The concentration of cytosolic Ca^{2+} ($[Ca^{2+}]_i$) is tightly controlled by Ca^{2+} transporters in the plasma membrane and intracellular Ca^{2+} stores. The transient receptor potential (TRP) proteins are novel class of Ca^{2+}-permeable cationic channels including six subfamilies, i.e., TRPC, TRPM, TRPV, TRPP, TRPML and TRPA. The canonical TRP (TRPC) is one of the subfamilies, which has been proposed as protein tyrosine kinase or G protein-coupled receptor-operated Ca^{2+} channels (ROCs) or internal Ca^{2+} store-operated channels (SOCs), which mediate the Ca^{2+} signalling pathway activated by many hormones and growth factors. TRPCs are ubiquitously distributed in the body and play essential roles in human physiology and pathophysiology [1, 2].

Ca^{2+} signalling is believed to play a central role in the signalling cascades of tumorigenesis and neoplastic progression by controlling gene expression, progression through the cell cycle, and DNA synthesis. The inhibitors of Ca^{2+}-dependent signalling suppress the proliferation of cancer cells *in vitro* and in solid tumors *in vivo* [3]. Store-operated Ca^{2+} influx is one of the Ca^{2+} entry pathways and closely related to cell proliferation and apoptosis. The importance of store-operated Ca^{2+} influx or capacitative Ca^{2+} influx in cancer development has been recognised for many years, however the role of TRP channels that act as the molecular constituents or subunits of SOCs or ROCs in cancer cell proliferation are still unclear [4]. In 2005, we demonstrated that TRPC channel is involved in cell proliferation, and 2-aminoethoxydiphenyl borate (2-APB) significantly inhibits the proliferation in HEK-293 cells. The mechanism is unrelated to its inhibitory action on inositol 1,4,5-trisphosphate receptors (IP_3R), since 2-APB also inhibits the proliferation of triple IP_3R knockout DT40 cells [5]. This suggests the direct involvement of SOCs or TRPC channels in cell proliferation. Recently, several studies have demonstrated the expression of TRPC in different types of cancer cells or cancer tissues, such as TRPC1, 3, 6 in breast cancer MCF7 cells [6] and liver cancer HepG2 [7], TRPC1, 3, 4 in prostate cancer LNCaP cells [8, 9], TRPC1, 4, 6, 7 in renal cell carcinoma [10], TRPC1, 3, 5, 6 in human malignant gliomas [11], TRPC1, 3-7 in neuroblastoma IMR-32 cells [12], TRPC3 in human astrocytoma 1321N1 cells [13], TRPC6 in esophageal and gastric cancer [14], TRPC3 in ovarian cancer [15], and TRPC1, 4 in basal cell carcinoma [16]. However, the detection of splicing activity of TRPCs and systematic examination of the role of each TRPC isoform in cancer growth has not been addressed.

Here we aimed to identify the expression of TRPCs and their splicing variants in human ovarian adenocarcinoma and the cancer-derived cell SKOV3, and determine the roles of TRPC isoforms in the regulation of cancer cell proliferation using TRPC siRNA interference and the pharmacological tools, such as the specific TRPC channel functional antibodies [5]. We also examined the colony growth of ovarian cancer cells by over-expressing TRPC isoforms. In addition, we compared the expression of TRPC genes in the human ovarian cancer tissues from patients with the normal ovarian tissues, and their involvement in ovarian cancer cell differentiation.

MATERIALS AND METHODS

Human Ovarian Cancer Tissues. Paraffin blocks of human ovarian adenocarcinoma tissue were obtained from patients undergoing ovariectomy at Hull and East Yorkshire NHS Trust (Hull, UK) with approval of the local ethics committee. The fresh ovarian cancer tissues were obtained from Qi Lu Hospital of Shandong University (Jinan, China) with ethical approval.

Cell Culture. Human ovarian adenocarcinoma cells (SKOV3, ATCC HTB-77) were purchased from LGC Promochem (Middlesex, UK). The SKOV3 cells were cultured in a flask with DMEM-F12 medium (Invitrogen, UK) supplemented with 10% fetal calf serum, 100 units/ml penicillin and 100 μg/ml streptomycin, and maintained at 37°C under 95% air and 5% CO_2.

RT-PCR and Real-time PCR. Total RNA was extracted from human ovarian tissues or cultured cells using Trizol reagent (Invitrogen, UK). The mRNA was reverse-transcribed to cDNA using M-MLV reserve transcriptase (RT) and random primers (Promega, UK). The primer set was designed across intron and the sequences were given in the supplementary Table 1. Non-template or non-RT was set as negative control, and the TRPC plasmid cDNAs or mouse brain cDNA were used as positive control. PCR products were detected on a 2 % agarose gel and confirmed by direct sequencing. Quantitative RT-PCR was performed using StepOne™ Real-Time PCR System (Applied Biosystems, UK). Each reaction volume was 10 μl, which contained 1 × Universal Master Mix (Applied Biosystems), 5 μl cDNA, 0.75 μl 300 nM forward primer, 0.75 μl 300 nM reverse primer. The human housekeeping gene GAPDH was used as an internal standard. Water was used as a non-template control. Non-reverse transcribed samples were run in parallel to confirm that positive results were not due to amplification of genomic DNA. The PCR cycle consisted of an initial cycle of 50 ˚C for 2 min followed by 95 ˚C for 10 minutes, then 50 repeated cycles of 95 ˚C for 15 s denaturation and 54 ˚C annealing temperature for 30 s, and primer extension at 72 ˚C for 30 s.

Antibodies and Western Blotting. Rabbit polyclonal anti-TRPC antibodies were generated against the extracellular third loop (E3) region near the channel pore [17] or targeting to C-terminus [18]. The specificity of E3-targeting antibodies (anti-TRPC1 (T1E3), anti-TRPC4 (T45E3), anti-TRPC5 (T5E3) and anti-TRPC6 (T367E3)) was tested by ELISA, Western blotting and functional assays [17]. The specific binding of E3-targeting antibodies was also confirmed by fluorescence activated cell sorting (FACS) (Fig. S1). The Western blotting procedure has been previously described [17].

Immunostaining. Cells were fixed with 4% paraformaldehyde and permeabilised by incubation in -20°C methanol for 1 minute and 0.1% Triton X-100 in phosphate buffered saline (PBS) for 1 hour at room temperature. For unpermeabilised staining, the steps for methanol and Triton X-100 were omitted. Cells were incubated in the appropriate TRPC primary antibodies (T1E3 at 1:500 dilution, T45E3, T367E3, anti-TRPC3 at 1:250 dilution) in PBS with 1% BSA at 4°C overnight. The anti-TRPC3 targeting C-terminus and the anti-TRPC6 targeting to N-terminus were purchased from Alomone Labs (Jerusalem, Israel) and used for comparison. The procedures for fluorescent staining and paraffin section staining using VECTASTAIN ABC kit (Vector laboratories) were similar to the previous reports [19]. Immunostaining was quantified by imaging software (Image-Pro Plus, Media Cybernetics, USA).

SiRNA Transfection. The TRPC siRNAs were purchased from Sigma-Aldrich (UK) (Supplementary Table 2). TRPC siRNAs were transfected into SKOV3 cells using Lipofectamine 2000 (Invitrogen, UK) [2]. The wells or dishes without siRNA (no siRNA) or with scramble siRNA (Sigma-Aldrich, UK) or non-specific pool siRNA were set as negative control in parallel. The Bcl-2 siRNA was used as positive control. For cell cycle experiment, SKOV3 cells were transfected with TRPC siRNAs using the Neon electroporation system (Invitrogen, UK). The cells were resuspended to a density of 5×10^6/ml and mixed with 200 nM siRNA, and then pulsed twice at 1,170 V for 30 ms in a 100 μl tip. After electroporation the cells were maintained in antibiotic-free medium for 72 h and harvested for flow cytometry assay.

TRPC cloning, plasmid construction and expression. TRPC1, TRPC1^{E9del} and TRPC6 tagged with monomeric cyan fluorescent protein (CFP) were subcloned into pcDNA4/TO vector (Invitrogen, UK). TRPC3 tagged with monomeric red fluorescent protein (mCherry) and TRPC4 (αβ, and ε isoforms) tagged with enhanced yellow fluorescent protein (EYFP) were also subcloned into pcDNA4/TO vector. The plasmid cDNA of each TRPC isoform was transfected into HEK293 T-REx cells (Invitrogen, UK) using Lipofectamine 200 0 and the expression was induced by tetracycline (1 μg/ml) and confirmed by fluorescent microscope examination. The channel activity was recorded by whole-cell patch clamp.

Cell Proliferation Assay and Colony Growth. Cell proliferation was determined using WST-1 assay (Roche, UK). This assay reflects the metabolic activity of the cultured cells. The overall cellular metabolic activity measured by optical absorption correlates well with the viable cell number in the culture dish/well. For colony growth, SKOV3 cells transfected with TRPC plasmid cDNAs using Lipofectamine 2000, and the cells were plated in 6-cm culture dishes at a density of 500 cells per dish to allow to form colonies after 3-8 days culture. The colonies were fixed with 25% methanol, stained with 0.5% crystal violet dye in PBS, and automatically counted by CellC software (Version 1.2, Tampere University of Technology, Finland). For soft agar colony assay, the bottom layer of agar (0.7 %) was prepared in a 35-mm culture dish with 1.5 ml of DMEM-F12 medium containing agar, 10% FBS, 50 μg/ml penicillin and 50 μg/ml streptomycin. After solidification of the bottom layer, SKOV3 cells were suspended in 1 ml medium containing 0.35% agar at a density of 5000 cells/ml and poured into the dish to form a second layer. The dish was kept at 4 ºC for 5 min and then the solidified second layer was covered with 1 ml medium to prevent the agar layer from drying out. The cells were incubated at 37°C in a humidified incubator and the top layer of medium was gently changed every 3 days. After 21 days of culture, the cells were stained with 0.005% crystal violet and the cell colonies with diameters >100 μm were counted under microscope with 4× objective.

Cell Cycle and Apoptosis Analyses. Simultaneous measurement of cell cycle and apoptosis was conducted using flow cytometric assay with propidium iodide staining as described by Riccardi and Nicoletti [20]. Briefly, SKOV3 cells at 70-80% confluency in a 100-mm culture dish were trypsinized, washed with PBS, fixed with 70% cold ethanol, incubated with DNA extraction buffer (0.2 M Na_2HPO_4, 0.004% Triton X-100, pH 7.8), treated with RNase (200 μg/ml), and stained with propidium iodide (20 μg/ml). The cells were then analysed with BD FACSCalibur Flow Cytometry System (Becton Dickinson, UK) with the CellQuest software. Events were counted at the limit of 20,000 or 10,000 for the drug-treated or siRNA-transfected groups. Cell debris was gated out according to the scatter plot and the percentages of cells at different phases of cell cycle were calculated based on the histogram plot of fluorescent intensities.

Reagents and Chemicals. 2-Aminoethoxydiphenyl borate (2-APB), SKF-96365, carbenoxolone, trypsin, all-*trans* retinoic acid, PCR primers, TRPC1, 4, 6 siRNAs and scramble siRNA were purchased from Sigma-Aldrich. TRPC3 siRNA was purchased from Santa Cruz Biotechnology (USA). Bcl-2 siRNA and pool siRNA were from Upstate Biotech (USA).

Statistical Analysis. Data are expressed as mean ± S.E.M. The statistical significance was analysed using ANOVA and the difference among the groups was assessed with Dunnett's *t*-test in the SPSS software. The triplicate wells (or 8 wells/column) were set for cell proliferation assay.

RESULTS

Expression of TRPCs in Human Ovarian Cancer SKOV3 Cells. The mRNA of TRPCs in ovarian cancer cells was detected by RT-PCR (Fig. 1A). TRPC1, TRPC3, TRPC4 and TRPC6 were positive in human ovarian adenocarcinoma SKOV3 cells, while TRPC5 and TRPC7 were undetectable in the cells although the primer sets used for TRPC5 and TRPC7 can amplify the plasmid cDNAs (Fig. 1B) or the total RNA extracted from mouse brain (Fig. S2). Two bands for TRPC1 were detected, suggesting splicing isoforms may exist in the cells.

The protein expression of TRPC channels was probed by western blotting (Fig. 1C). The protein bands for TRPC1, TRPC3, TRPC4 and TRPC6 were detected using anti-TRPC1 (T1E3), anti-TRPC3, anti-TRPC4 (T45E3) and anti-TRPC6 (T367E3) antibodies, respectively, while no specific band was detected using preimmune serum or antibody pre-absorbed with antigenic peptide. Same size of TRPC6 protein band was detected by anti-TRPC6 antibody targeting the N-terminus (Fig 1C).

Identification of TRPC Spliced Variants. The expression of TRPC spliced variants in SKOV3 cells were examined by RT-PCR using specific primer sets across introns. The spliced variant of TRPC1 with exon 3 deletion (TRPC1β) was detected using the primer set across exon 3 (P1). The band density of TRPC1β is much stronger than the full-length isoform (TRPC1α)(Fig. 2A), suggesting that the β-isoform is highly expressed in the cancer cells. Using the primer set across the exon 9 and 10 (P3), a novel spliced variant of TRPC1 with exon 9 deletion ($TRPC1^{E9del}$) was identified (GenBank accession No. GQ293239). The existence of $TRPC1^{E9del}$ was also confirmed by using the TRPC1 primer set across exon 9 (P4). The band density of the $TRPC1^{E9del}$ was less abundant than the non-spliced TRPC1 isoform in the region. The deletion of exon 9 did not cause open reading frame shift, suggesting this new spliced isoform may have a channel pore domain and C-terminus that seen in αor β isoforms. Interestingly, the $TRPC1^{E9del}$ isoform was absent in normal mouse brain tissue (Fig. S2) and vascular smooth muscle cells or arteries detected by same primer set (P4) [21]. These data suggested that TRPC1 is actively spliced in cancer cells. In addition, we also examined the possibility for other splicing regions using primer set P2 and P5, and the primer combination ranged from exon 1 to exon 13, but no other splicing site was identified.

Full-length human TRPC3 has 12 exons and a 58-base pair insert between exon 2 and exon 3. Using primer set across exon 2-5 (P1), or exon 3-5 (P2), exon 5-6 (P3) and exon 8-9 (P4), single PCR band with the expected size was detected. TRPC3 has an isoform with an extended N-terminus (TRPC3a) [22], so we detected this isoform using primer set across exon 1-5 (P0). As shown in Fig. 2B, a band with an expected size of 1405 bp was detected, suggesting the TRPC3a isoform existed in the SKOV3 cells. We also amplified the regions of exon 5-9 and exon 8-12, but no other spliced isoforms were found in SKOV3 cells.

Eight spliced variants of human TRPC4 have been reported including α, β, γδ, ε, ζ, η and an unnamed isoform truncated at exon 6. Based on the sequence alignment (Fig. S3), the αβ, γ, δ, ε and ζ isoforms of TRPC4 have 100 % identity for the region from exon 1 to exon 7 except TRPC4ζ that has exon 3 deletion. The η-isoform has an early stop code due to open reading frame shift at the end of exon 3. Using primer set P1 and P4, TRPC4 was positive in SKOV3 cells with the size of 740 bp and 519 bp, respectively. However, the ζ-isoform with exon 3 deletion was undetectable using the primer set across exon 1-5 (P2) (data not shown). The ε-isoform of TRPC4 was also undetectable with the forward primer in exon 7 and the ε-isoform specific reverse primer. However, two bands were detected with an expected

size of 428 bp and 623 bp using the primer set (P3). The smaller band is specific for TRPC4γ and the bigger band is the unspliced isoforms of TRPC4 without exon 8 deletion. Similarly, two bands were detected if the primer set across the exon 8 alone (P6) (data not shown) was used, suggesting the TRPC4γ and other isoforms co-existed in the SKOV3 cells. To further distinguish the TRPC4 isoforms, the primer set (P7) amplifying exon 7 to exon 12 were used, the detected band with a predicted size of 956 bp is α-isoform, and the small band (704 bp) for the β-isoform (Fig. 2C). In addition, we also examined the possibility for other splicing regions using the forward and reverse primer combinations ranged from exon 1 to exon 11, and no other splicing region was found. These data indicated that α-, β- and γ-isoforms of TRPC4 coexist in the SKOV3 cells.

There are 13 exons for human TRPC6. Three bands were detected using primer set (P1) to amplify exon 1-5. The size for the full-length TRPC6 is 1222 bp. The two spliced isoforms with exon 3 deletion is 1039 bp and with exon 3 and 4 deletion is 874 bp, respectively. No spliced region was found between exon 8 to exon 13 (Fig. 2D).

Functional Properties of TRPC Isoforms. We examined the functional properties of TRPC isoforms using whole-cell patch recording. TRPC1, TRPC1^{E9del}, TRPC3, TRPC4α,TRPC4β, TRPC4ε and TRPC6 were inducibly expressed in HEK293 T-REx cells using pcDNA4/TO expression system. TRPC1 and TRPC1^{E9del} were mainly located intracellularly (See Fig. 6C) and the whole-cell current was small (data not shown), however the currents for TRPC3, TRPC4α and TRPC6 were robust and significantly evoked by trypsin via G protein-coupled receptor activation and blocked by 2-APB (Fig. S4). We compared the functionality of TRPC4α, TRPC4β and TRPC4ε isoforms. TRPC4α and TRPC4β showed a similar current-voltage (*IV*) relationship and both of them were activated by Gd^{3+} and blocked by 2-APB, however the current for TRPC4ε was much smaller and the *IV* curve was linear, which is different from the *IV* curves for TRPC4α and TRPC4β with double rectifications (Fig. S5). These results suggest the potential functional differences among the TRPC isoforms due to the different subcellular distribution and channel properties.

Ovarian Cancer Cell Growth Regulated by TRPC Channel Modulators. 2-APB is a non-selective blocker of TRPC channels [5]. The blockade of TRPC channels by 2-APB significantly inhibited the SKOV3 proliferation in a concentration-dependent manner with an EC_{50} of 5.9 μM (Fig. 3A). Since 2-APB has been shown to inhibit gap junctional channels, which might contribute to the anti-proliferative effect [23, 24], we pretreated the SKOV3 cells with carbenoxolone, a gap junctional blocker, to pharmacologically dissect out the contribution of TRPC channels. Carbenoxolone at 200 μM and 400 μM significantly inhibited the cell proliferation (Fig. 3B), but the anti-proliferative effect of 2-APB was still reserved in the presence of carbenoxolone (Fig.3C), suggesting that the anti-proliferative effect of 2-APB could be due to the inhibition on TRPC channels. We also observed the effect of SKF-96365, another non-specific TRPC channel blocker. SKF-96365 significantly inhibited the cell proliferation of SKOV3 in a concentration-dependent manner with an EC_{50} of 14.5 μM (Fig. 3D), however Gd^{3+} which can differentially activate TRPC4 and TRPC5 channels showed a stimulating effect on cell proliferation (Fig. 3E). In addition, we tested the channel activator trypsin on cell proliferation. Trypsin significantly stimulated TRPC3, 4 and 6 channels as shown in Fig. S4, which can be explained by the mechanism of protease-activated receptor activation. Incubation with trypsin promoted the cancer cell proliferation (Fig. 3F). These data suggest the importance of TRPC channel activity in regulating ovarian cancer cell growth, and the channel blockers could have the potential for anti-cancer therapy.

Role of TRPC Isoforms in Ovarian Cancer Cell Proliferation. To identify the role of individual TRPC isoforms on the cancer cell proliferation, SKOV3 cells were incubated with E3-targeting TRPC

functional antibodies that can specifically inhibit Ca^{2+} influx via TRPC channels [17, 21]. The specificity of antibody binding was confirmed by ELISA and FACS as shown in Fig. S1. The blockade of TRPC1, TRPC4 and TRPC6 channels by T1E3, T45E3 and T367E3 significantly decreased the cancer cell proliferation (Fig. 4A), but T5E3, which can block TRPC5 channel only, had no effect on cell proliferation, further suggesting the lack of TRPC5 expression in SKOV3 cells.

The isoform-specific TRPC siRNAs were used to further demonstrate the role of TRPCs in cancer cell proliferation. The downregulation of TRPCs by siRNAs was confirmed by real-time PCR (data not shown). There was no difference among the groups transfected with scramble siRNA, pool siRNA and mock control transfection (no siRNA) on SKOV3 cell proliferation. However, the cell proliferation was significantly inhibited by the transfection with TRPC1, TRPC3, TRPC4 and TRPC6 siRNAs for 48 hours. Bcl-2 siRNA, which targets the anti-apoptotic Bcl-2 gene, was used as a positive control, also significantly inhibited cell proliferation (Fig. 4B). These results were similar to the observations using specific anti-TRPC functional antibodies, suggesting that the silencing of TRPC channel expression is important for the inhibition of cancer cell proliferation.

Overexpression of TRPC Isoforms Promotes Cancer Colony Growth. There are no specific siRNAs or blocking antibody tools targeting to individual spliced variants of TRPCs, therefore we overexpressed the TRPC isoforms to further confirm the role of TRPC in ovarian cancer growth. SKOV3 cells were transfected with the plasmid TRPC and $TRPC1^{E9del}$ cDNAs and the cancer cell colony formation was observed. As shown in Figure 4C-D, the large colony number (>2 mm^2) was greatly increased in the groups transfected with TRPC1, $TRPC1^{E9del}$, TRPC3, TRPC4 and TRPC6. We also examined the cancer colony growth using soft agar assay. The number of larger colony with a diameter >100 μm was much higher in the groups transfected with TRPC1, $TRPC1^{E9del}$, TRPC3, TRPC4 and TRPC6 than that in the vector control group, which further suggested the involvement of TRPCs in the ovarian cancer development.

Effects of TRPC Channel Blocker and Gene Silencing on Cell Cycle. The ovarian cancer cell cycle was determined by FACS using propidium iodide staining procedure [20]. Incubation with the non-selective TRPC channel blocker SKF-96365 (10 μM) substantially increased the G_2/M phase and decreased the G_0/G_1 phase in the SKOV3 cells (Fig. 5A), which was accorded to the previous report [15]. To further observed the effects of individual TRPC genes on cell cycle progress, the SKOV3 cells were transfected with TRPC siRNAs. We found that more SKOV cells were arrested at G_2/M phase after transfection with siTRPC1, siTRPC4, siTRPC3, and siTRPC6 for 72 hours comparing with the control group transfected with scramble siRNA (Fig. 5B), suggesting that the downregulation of TRPC gene expression can arrest the cell cycle progression through G_2/M to G_1. Unlike the channel blocker SKF-96365, the contribution of TRPC gene silencing on apoptosis was small (Fig. 5). The down-regulation of TRPC expression did not significantly change the apoptosis in ovarian cancer.

Differentiation-associated TRPC Expression. The expression of TRPC was examined by RT-PCR using ovarian cancer tissues from five patients with undifferentiated ovarian serous papillary adenocarcinoma. The five normal ovarian tissues obtained from patients at a similar age but without ovarian cancer were used as control. The mRNAs for TRPC1, TRPC3, TRPC4 and TRPC6 were positive in normal and ovarian cancer tissues. However, the mRNA level of TRPC1, TRPC3, TRPC4 and TRPC6 was significantly lower in the undifferentiated ovarian cancer than that in normal ovarian tissue (Fig. 6), suggesting that the expression of TRPCs was down-regulated in the cell type of undifferentiated ovarian cancer.

We also examined the protein expression of TRPCs in human ovarian adenocarcinoma tissues by immunostaining. The paraffin-embedded ovarian cancer tissue sections were stained using Vectastain ABC systems. TRPC1, TRPC4 and TRPC6 were positively stained by T1E3, T45E3 and T367E3 antibodies, while the control staining with preimmune serum or without primary anti-TRPC antibodies was negative. The staining pattern for TRPC6 was similar to that by an anti-TRPC6 antibody targeting to the N-terminus (Fig. 7A). We compared the immunostaining density between the undifferentiated or poorly differentiated (Grade 3) and well differentiated (Grade 1-2) ovarian tissue sections. The expression of TRPC1, TRPC4 and TRPC6 were significantly lower in the undifferentiated ovarian cancer tissues (Fig. 7B).

TRPC Expression Enhanced by all-*trans* Retinoic Acid (atRA). AtRA is a potent regulator for cell differentiation in a variety of cell types and plays an important role in anticancer therapy by affecting gene transcription [25, 26]. To further examine the association of TRPC in ovarian cancer cell differentiation, we tested the effect of atRA on TRPC expression. Using real-time RT-PCR, we found that the mRNA level for TRPC1, TRPC3, TRPC4, and TRPC6 was significantly increased in the SKOV3 cells treated with 1 μM atRA for 5 days (Fig. 7C), suggesting that TRPC expression is associated with atRA-induced cell differentiation.

Subcellular Distribution of TRPC Isoforms. The subcellular distribution of TRPC channel proteins was investigated in the SKOV3 cells and the TRPC-transfected cells. SKOV3 cells were stained with anti-TRPC1 (T1E3), anti-TRPC3, anti-TRPC4 (T45E3) and anti-TRPC6 (T367E3) antibodies. TRPC1 was more evident in the cytosol, but TRPC3, TRPC4 and TRPC6 were apparent in the plasma membrane (Fig. 7D(i)). The cultured SKOV3 had an irregular and very flat cell shape and tightly attached onto the coverslips, so it was hard to obtain a Z-section with a typical imaging for plasma membrane staining. Therefore, the unpermeabilized staining was also performed for TRPC1, TRPC4 and TRPC6 using extracellular binding antibodies, and the stainings were also positive (Fig. S6). Due to the lack of TRPC spliced variant-specific antibodies, it is impossible to see the subcellular localization of $TRPC1^{E9del}$ and TRPC4 isoforms in the native ovarian cancer cells, therefore, we explored the subcellular localization in the HEK-293 T-REx cells by over-expressing the isoforms tagged with fluorescence proteins. $TRPC1^{E9del}$ protein was mainly intracellularly located, which is similar to that of the full-length TRPC1. However, channel proteins for TRPC3, TRPC4α,TRPC4β, TRPC4ε and TRPC6 were evident in the plasma membrane (Fig. 7D(ii)).

DISCUSSION

We have shown that TRPC1, TRPC3, TRPC4 and TRPC6 exist in the tissue section of human ovarian adenocarcinoma and the ovarian adenocarcinoma-derived cell line SKOV3. We have also shown that several spliced variants of TRPC1, TRPC3, TRPC4 and TRPC6 co-express in the ovarian cancer cells. In addition, a new TRPC1 spliced variant with exon 9 deletion has been identified in this study. Blockade of TRPC channel activity by 2-APB, SKF-96365, or by TRPC isoform-specific functional antibodies or by the transfection with TRPC siRNAs significantly inhibits the cancer cell proliferation, whilst the increase of TRPC channel activity by G protein-coupled receptor activation promotes the ovarian cancer cell growth. Overexpression of TRPC genes also increases ovarian cancer colony growth. Moreover, the expression in undifferentiated human ovarian cancer is significantly lower than in normal ovarian tissues. These findings are novel and important for understanding the roles of TRPC channels in ovarian cancer development.

TRPC channels have been identified in many cell types [2, 18, 27, 28]. These channels are differentially expressed at different stages of stem cell development, which may reflect their importance in cell differentiation [29, 30]. On the other hand, the thapsigargin-induced store-operated Ca^{2+} influx is higher in tumour cells than that in normal cells [31], which further suggests the relevance of TRPC channels or store-operated channel molecules to cancer development. In this study, we have systematically detected the TRPC channels and their splice variants, and found that multiple TRPCs and their spliced isoforms exist in human ovarian cancer. TRPC1 has been suggested as a store-operated channel subunit and actively associates with other TRPC isoforms, such as TRPC1/4 or TRPC1/5 [18, 32], or interacts with other channel proteins, such as ORAI1 or STIM1 [33], to constitute the heteromultimeric store-operated channels or channel complexes, which could be main molecular components in native cells. Interestingly, the existence of several spliced isoforms of TRPCs in a cell suggests the possibility of functional interaction or regulation on the channel activity. TRPC1γ1 and TRPC1γ2 have been reported in human myometrial cells [34], but none of them have been detected in the ovarian cancer cells, and no inserts found between exon 8 to exon 10. Instead, we have identified a new TRPC1 isoform with exon 9 deletion, suggesting this TRPC1 spliced isoform lacks transmembrane segment 4 (S4). $TRPC1^{E9del}$ is mainly distributed in the cytosol with a similar subcellular distribution pattern to the full length TRPC1. The nuclear membrane localisation for TRPC1 and $TRPC^{E9del}$ is also evident. However, other isoforms including TRPC3, TRPC4α,TRPC4β, TRPC4ε and TRPC6 are located in the plasma membrane, suggesting the potential functional difference between TRPC1 and other TRPC isoforms. Since the current of over-expressed TRPC1 is small and difficult to be distinguished from the endogenous current, we have not compared the biophysical difference between TRPC1 and $TRPC1^{E9del}$. However, we believe that the $TRPC1^{E9del}$ is a functional subunit, because the colony growth is significantly increased by the overexpression of $TRPC1^{E9del}$, although the underling mechanism is unclear and needed to be further investigated. Moreover, the spliced isoforms of TRPC1 with exon 2 and exon 3 deletion have been described in mice by Sakura & Ashcroft [35], but this splicing activity has not been found in human SKOV3 cells. TRPC3 and TRPC6 have a high similarity in sequence. Both of them have been demonstrated as receptor-operated channels that mediate the diacylglycerol-induced Ca^{2+} influx, although TRPC3 may also have store-operated channel properties [36, 37]. In addition, co-existence of several TRPC4 isoforms in the SKOV cells could be important for protein interactions among the TRPC isoforms that may be required for precisely regulating the functionality of Ca^{2+} permeable channel complexes in cancer cells, and thus control cell growth. Indeed, some spliced TRPC isoforms have been demonstrated as an inhibitory subunit for TRPC homomultimeric channels in HEK-293 cells if co-overexpressed with the full-length isoforms [38, 39]. We also found that the channel property of TRPC4ε is different from other TRPC4 isoforms. Further investigation is needed to explore the functional difference among the alternative splicing of TRPCs in cancer development.

The expression level of individual TRPCs in different type of cancer cells or cancer tissues are variable, suggesting the differential expression of TRPCs in cancer cells [4, 30]. We also found such differences in our study, such as TRPC4 expressed in SKOV3, but not in breast cancer MCF7 cells (data not shown). In addition, the expression level may depend on the differentiation status of the cancer cells, because we found that the undifferentiated ovarian cancer has lower expression of TRPC1, TRPC4 and TRPC6, which is consistent to the observation of low level of TRPC4 and TRPC6 in immature stem cells [29]. This observation was further confirmed in the *in vitro* experiment using the cell differentiation regulator atRA. It has been reported that atRA at 1 μM inhibited SKOV3 cell proliferation and phenotype, although the ovarian cell line is less sensitive to atRA treatment [40, 41]. We were unable to compare the expression among the different ovarian cancer types and different grades of differentiation in this study due to the source of fresh ovarian sample, however, a large scale collaborative study is needed in the future.

The anti-proliferative effect of 2-APB has been demonstrated in gastric cancer cell lines [42], colon cancer cell [43] and human hepatoma cells [44]. Here we found that the effect of 2-APB was not altered by the gap junctional channel blocker, carbenoxolone, further suggesting that the anti-proliferative action of 2-APB is due to the inhibition on store-operated channels. 2-APB and SKF-96365 are broad-spectrum TRPC channel blockers and cannot distinguish the contribution of individual TRPC isoforms, therefore the isoform-specific functional antibody tools were used in this study. The specificity of the antibodies has been confirmed by ELISA, western blotting, *in vitro* functional testing on Ca^{2+} influx and FACS-based assay. The block on TRPC1, TRPC4 and TRPC6 channels by E3-targeting functional antibodies caused a significant inhibition of cell proliferation, suggesting that TRPC1, TRPC4 and TRPC6 are important for cancer cell proliferation. This effect was further confirmed by the application of TRPC isoform-specific siRNAs. The M phase was mainly arrested for the cell cycle progression, which is similar to the study using TRPC3 siRNA alone [15].

We have not examined other TRP subfamilies related to cancer, such as TRPM1 in melanoma [4], TRPM7 in human retinoblastoma cells [45] and human head and neck carcinoma cells [46], TRPM8 and TRPV6 in prostate cancer [30, 47]. The potential contribution of other molecules or subunits of store-operated channels, such as STIM and ORAI proteins and MS4A12 [48, 49], may also be important in the regulation of store-operated Ca^{2+} signalling in cancer.

Cell apoptosis has been suggested to be related to store operated channel [50]. Thapsigargin can induce apoptosis of prostate cancer cells, but this effect cannot be prevented by an intracellular Ca^{2+} chelator, suggesting that the increase of cytosol Ca^{2+} is unnecessary for apoptosis [50]. We found that the non-selective channel blocker 2-APB (data not shown) and SKF-96365 can evoke ovarian cancer cell apoptosis, but the specific TRPC siRNAs do not significantly change the apoptosis, suggesting the TRPC channels may be less important in the regulation of cancer cell apoptosis, therefore we have not explored the details of TRPCs in cancer cell apoptosis in this study.

Ca^{2+} is a key signal for cell growth or death. The specific activation of pathways and channels for precisely regulating Ca^{2+} influx is important for both normal and cancer cells. We found that TRPC1, TRPC3, TRPC4 and TRPC6 channels are expressed in ovary cancer, and the splicing variants of TRPCs are highly expressed in the cancer cells, which is important for understanding the molecular pathways for Ca^{2+} entry. Inhibition of these channel activity or expression level leads to the anti-proliferative effect, so the TRPC channels should be considered as potential targets for cancer therapy. In addition, the lower expression of TRPC or its isoforms could be developed negative prognostic biomarkers for certain type of cancer, such as the undifferentiated type of ovarian cancer.

ACKNOWLEDGMENTS

We thank J Wake and LA Madden for technical support. This work was supported in part by the HYMS Priming Award to S.Z.X.. B.Z. was supported by China Scholarship Council and the university studentship. X.Y. and C.Y. were supported by National Natural and Science Foundation of China.

ABBREVIATIONS

2-APB = 2-Aminoethoxydiphenyl borate

atRA = all-*trans* retinoic acid
CFP = cyan fluorescent protein
EYFP = enhanced yellow fluorescent protein
FACS = fluorescence activated cell sorting
GAPDH = glyceraldehyde 3-phosphate dehydrogenase
IP_3R = inositol 1,4,5-trisphosphate receptor
PBS = phosphate buffered saline
RT = reserve transcriptase
ROCs = receptor-operated Ca^{2+} channels
SOCs = store-operated Ca^{2+} channels
TRPC = transient receptor potential canonical

SUPPORTIVE/SUPPLEMENTARY MATERIAL

Supplementary methods: Fluorescence activated cell sorting (FACS) and electrophysiological recordings.
Figure S1: Specific binding of functional anti-TRPC Antibodies
Figure S2: RT-PCR detection of TRPC1-7 in mouse brain
Figure S3: Sequence alignment of human TRPC4 isoforms
Figure S4: Whole-cell current of TRPC isoforms overexpressing in HEK293 T-REx cells.
Figure S5: Functional properties of TRPC4 splicing isforms.
Figure S6: Impermeable staining of SKOV3 with anti-TRPC antibodies.
Supplementary Table 1: Primer sequences for RT-PCR
Supplementary Table 2: Sequences of TRPC siRNAs

REFERENCES

[1] Clapham DE. TRP channels as cellular sensors. *Nature* **2003**,*426*, 517-524.

[2] Xu SZ; Sukumar P; Zeng F; Li J; Jairaman A; English A; Naylor J; Ciurtin C; Majeed Y; Milligan CJ; Bahnasi YM; Al-Shawaf E; Porter KE; Jiang LH; Emery P; Sivaprasadarao A; Beech DJ. TRPC channel activation by extracellular thioredoxin. *Nature* **2008**,*451*, 69-72.

[3] Holmuhamedov E; Lewis L; Bienengraeber M; Holmuhamedova M; Jahangir A; Terzic A. Suppression of human tumor cell proliferation through mitochondrial targeting. *Faseb J* **2002**,*16*, 1010-1016.

[4] Prevarskaya N; Zhang L; Barritt G. TRP channels in cancer. *Biochim Biophys Acta* **2007**,*1772*, 937-946.

[5] Xu SZ; Zeng F; Boulay G; Grimm C; Harteneck C; Beech DJ. Block of TRPC5 channels by 2-aminoethoxydiphenyl borate: a differential, extracellular and voltage-dependent effect. *Br J Pharmacol* **2005**,*145*, 405-414.

[6] Aydar E; Yeo S; Djamgoz M; Palmer C. Abnormal expression, localization and interaction of canonical transient receptor potential ion channels in human breast cancer cell lines and tissues: a potential target for breast cancer diagnosis and therapy. *Cancer Cell Int* **2009**,*9*, 23.

[7] El Boustany C; Bidaux G; Enfissi A; Delcourt P; Prevarskaya N; Capiod T. Capacitative calcium entry and transient receptor potential canonical 6 expression control human hepatoma cell proliferation. *Hepatology* **2008**,*47*, 2068-2077.

[8] Thebault S; Flourakis M; Vanoverberghe K; Vandermoere F; Roudbaraki M; Lehen'kyi V; Slomianny C; Beck B; Mariot P; Bonnal JL; Mauroy B; Shuba Y; Capiod T; Skryma R; Prevarskaya N. Differential role of transient receptor potential channels in Ca2+ entry and proliferation of prostate cancer epithelial cells. *Cancer Res* **2006**,*66*, 2038-2047.

[9] Pigozzi D; Ducret T; Tajeddine N; Gala JL; Tombal B; Gailly P. Calcium store contents control the expression of TRPC1, TRPC3 and TRPV6 proteins in LNCaP prostate cancer cell line. *Cell Calcium* **2006**,*39*, 401-415.

[10] Veliceasa D; Ivanovic M; Hoepfner FT; Thumbikat P; Volpert OV; Smith ND. Transient potential receptor channel 4 controls thrombospondin-1 secretion and angiogenesis in renal cell carcinoma. *Febs J* **2007**,*274*, 6365-6377.

[11] Bomben VC; Sontheimer HW. Inhibition of transient receptor potential canonical channels impairs cytokinesis in human malignant gliomas. *Cell Prolif* **2008**,*41*, 98-121.

[12] Nasman J; Bart G; Larsson K; Louhivuori L; Peltonen H; Akerman KE. The orexin OX1 receptor regulates Ca2+ entry via diacylglycerol-activated channels in differentiated neuroblastoma cells. *J Neurosci* **2006**,*26*, 10658-10666.

[13] Nakao K; Shirakawa H; Sugishita A; Matsutani I; Niidome T; Nakagawa T; Kaneko S. Ca2+ mobilization mediated by transient receptor potential canonical 3 is associated with thrombin-induced morphological changes in 1321N1 human astrocytoma cells. *J Neurosci Res* **2008**,*86*, 2722-2732.

[14] Cai R; Ding X; Zhou K; Shi Y; Ge R; Ren G; Jin Y; Wang Y. Blockade of TRPC6 channels induced G2/M phase arrest and suppressed growth in human gastric cancer cells. *Int J Cancer* **2009**,*125*, 2281-2287.

[15] Yang SL; Cao Q; Zhou KC; Feng YJ; Wang YZ. Transient receptor potential channel C3 contributes to the progression of human ovarian cancer. *Oncogene* **2009**.

[16] Beck B; Lehen'kyi V; Roudbaraki M; Flourakis M; Charveron M; Bordat P; Polakowska R; Prevarskaya N; Skryma R. TRPC channels determine human keratinocyte differentiation: new insight into basal cell carcinoma. *Cell Calcium* **2008**,*43*, 492-505.

[17] Xu SZ; Zeng F; Lei M; Li J; Gao B; Xiong C; Sivaprasadarao A; Beech DJ. Generation of functional ion-channel tools by E3 targeting. *Nat Biotechnol* **2005**,*23*, 1289-1293.

[18] Xu SZ; Muraki K; Zeng F; Li J; Sukumar P; Shah S; Dedman AM; Flemming PK; McHugh D; Naylor J; Cheong A; Bateson AN; Munsch CM; Porter KE; Beech DJ. A sphingosine-1-phosphate-activated calcium channel controlling vascular smooth muscle cell motility. *Circ Res* **2006**,*98*, 1381-1389.

[19] Kumar B; Dreja K; Shah SS; Cheong A; Xu SZ; Sukumar P; Naylor J; Forte A; Cipollaro M; McHugh D; Kingston PA; Heagerty AM; Munsch CM; Bergdahl A; Hultgardh-Nilsson A; Gomez MF; Porter KE; Hellstrand P; Beech DJ. Upregulated TRPC1 channel in vascular injury in vivo and its role in human neointimal hyperplasia. *Circ Res* **2006**,*98*, 557-563.

[20] Riccardi C; Nicoletti I. Analysis of apoptosis by propidium iodide staining and flow cytometry. *Nat Protoc* **2006**,*1*, 1458-1461.

[21] Xu SZ; Beech DJ. TrpC1 is a membrane-spanning subunit of store-operated Ca(2+) channels in native vascular smooth muscle cells. *Circ Res* **2001**,*88*, 84-87.

[22] Yildirim E; Kawasaki BT; Birnbaumer L. Molecular cloning of TRPC3a, an N-terminally extended, store-operated variant of the human C3 transient receptor potential channel. *Proc Natl Acad Sci U S A* **2005**,*102*, 3307-3311.

[23] Harks EG; Camina JP; Peters PH; Ypey DL; Scheenen WJ; van Zoelen EJ; Theuvenet AP. Besides affecting intracellular calcium signaling, 2-APB reversibly blocks gap junctional coupling in confluent monolayers, thereby allowing measurement of single-cell membrane currents in undissociated cells. *Faseb J* **2003**,*17*, 941-943.

[24] Vinken M; Vanhaecke T; Papeleu P; Snykers S; Henkens T; Rogiers V. Connexins and their channels in cell growth and cell death. *Cell Signal* **2006**,*18*, 592-600.

[25] Kaiser PC; Korner M; Kappeler A; Aebi S. Retinoid receptors in ovarian cancer: expression and prognosis. *Ann Oncol* **2005**,*16*, 1477-1487.

[26] Um SJ; Lee SY; Kim EJ; Han HS; Koh YM; Hong KJ; Sin HS; Park JS. Antiproliferative mechanism of retinoid derivatives in ovarian cancer cells. *Cancer Lett* **2001**,*174*, 127-134.

[27] Flemming R; Xu SZ; Beech DJ. Pharmacological profile of store-operated channels in cerebral arteriolar smooth muscle cells. *Br J Pharmacol* **2003**,*139*, 955-965.

[28] Riccio A; Medhurst AD; Mattei C; Kelsell RE; Calver AR; Randall AD; Benham CD; Pangalos MN. mRNA distribution analysis of human TRPC family in CNS and peripheral tissues. *Brain Res Mol Brain Res* **2002**,*109*, 95-104.

[29] den Dekker E; Molin DG; Breikers G; van Oerle R; Akkerman JW; van Eys GJ; Heemskerk JW. Expression of transient receptor potential mRNA isoforms and Ca(2+) influx in differentiating human stem cells and platelets. *Biochim Biophys Acta* **2001**,*1539*, 243-255.

[30] Bodding M. TRP proteins and cancer. *Cell Signal* **2007**,*19*, 617-624.

[31] Kovacs GG; Zsembery A; Anderson SJ; Komlosi P; Gillespie GY; Bell PD; Benos DJ; Fuller CM. Changes in intracellular Ca2+ and pH in response to thapsigargin in human glioblastoma cells and normal astrocytes. *Am J Physiol Cell Physiol* **2005**,*289*, C361-371.

[32] Strubing C; Krapivinsky G; Krapivinsky L; Clapham DE. TRPC1 and TRPC5 form a novel cation channel in mammalian brain. *Neuron* **2001**,*29*, 645-655.

[33] Ong HL; Cheng KT; Liu X; Bandyopadhyay BC; Paria BC; Soboloff J; Pani B; Gwack Y; Srikanth S; Singh BB; Gill D; Ambudkar IS. Dynamic assembly of TRPC1-STIM1-Orai1 ternary complex is involved in store-operated calcium influx. Evidence for similarities in store-operated and calcium release-activated calcium channel components. *J Biol Chem* **2007**,*282*, 9105-9116.

[34] Yang M; Gupta A; Shlykov SG; Corrigan R; Tsujimoto S; Sanborn BM. Multiple Trp isoforms implicated in capacitative calcium entry are expressed in human pregnant myometrium and myometrial cells. *Biol Reprod* **2002**,*67*, 988-994.

[35] Sakura H; Ashcroft FM. Identification of four trp1 gene variants murine pancreatic beta-cells. *Diabetologia* **1997**,*40*, 528-532.

[36] Estacion M; Li S; Sinkins WG; Gosling M; Bahra P; Poll C; Westwick J; Schilling WP. Activation of human TRPC6 channels by receptor stimulation. *J Biol Chem* **2004**,*279*, 22047-22056.

[37] Venkatachalam K; van Rossum DB; Patterson RL; Ma HT; Gill DL. The cellular and molecular basis of store-operated calcium entry. *Nat Cell Biol* **2002**,*4*, E263-272.

[38] Schaefer M; Plant TD; Stresow N; Albrecht N; Schultz G. Functional differences between TRPC4 splice variants. *J Biol Chem* **2002**,*277*, 3752-3759.

[39] Satoh E; Ono K; Xu F; Iijima T. Cloning and functional expression of a novel splice variant of rat TRPC4. *Circ J* **2002**,*66*, 954-958.

[40] Hanna EA; Umhauer S; Roshong SL; Piechocki MP; Fernstrom MJ; Fanning JD; Ruch RJ. Gap junctional intercellular communication and connexin43 expression in human ovarian surface epithelial cells and ovarian carcinomas in vivo and in vitro. *Carcinogenesis* **1999**,*20*, 1369-1373.

[41] Guruswamy S; Lightfoot S; Gold MA; Hassan R; Berlin KD; Ivey RT; Benbrook DM. Effects of retinoids on cancerous phenotype and apoptosis in organotypic cultures of ovarian carcinoma. *J Natl Cancer Inst* **2001**,*93*, 516-525.

[42] Sakakura C; Miyagawa K; Fukuda K; Shimomura K; Takemura M; Takagi T; Kin S; Nakase Y; Fujiyama J; Mikoshiba K; Okazaki Y; Hayashizaki Y; Hagiwara A; Yamagishi H. [Possible involvement of inositol 1, 4, 5-trisphosphate receptor type 3 (IP3R3) in the peritoneal dissemination of gastric cancers]. *Gan To Kagaku Ryoho* **2003**,*30*, 1784-1787.

[43] Kazerounian S; Pitari GM; Shah FJ; Frick GS; Madesh M; Ruiz-Stewart I; Schulz S; Hajnoczky G; Waldman SA. Proliferative signaling by store-operated calcium channels opposes colon cancer cell cytostasis induced by bacterial enterotoxins. *J Pharmacol Exp Ther* **2005**,*314*, 1013-1022.

[44] Enfissi A; Prigent S; Colosetti P; Capiod T. The blocking of capacitative calcium entry by 2-aminoethyl diphenylborate (2-APB) and carboxyamidotriazole (CAI) inhibits proliferation in Hep G2 and Huh-7 human hepatoma cells. *Cell Calcium* **2004**,*36*, 459-467.

[45] Hanano T; Hara Y; Shi J; Morita H; Umebayashi C; Mori E; Sumimoto H; Ito Y; Mori Y; Inoue R. Involvement of TRPM7 in cell growth as a spontaneously activated Ca2+ entry pathway in human retinoblastoma cells. *J Pharmacol Sci* **2004**,*95*, 403-419.

[46] Jiang J; Li MH; Inoue K; Chu XP; Seeds J; Xiong ZG. Transient Receptor Potential Melastatin 7 like Current in Human Head and Neck Carcinoma Cells: Role in Cell Proliferation. *Cancer Res* **2007**,*67*, 10929-10938.

[47] Vanden Abeele F; Shuba Y; Roudbaraki M; Lemonnier L; Vanoverberghe K; Mariot P; Skryma R; Prevarskaya N. Store-operated Ca2+ channels in prostate cancer epithelial cells: function, regulation, and role in carcinogenesis. *Cell Calcium* **2003**,*33*, 357-373.

[48] Koslowski M; Sahin U; Dhaene K; Huber C; Tureci O. MS4A12 is a colon-selective store-operated calcium channel promoting malignant cell processes. *Cancer Res* **2008**,*68*, 3458-3466.

[49] Prakriya M; Feske S; Gwack Y; Srikanth S; Rao A; Hogan PG. Orai1 is an essential pore subunit of the CRAC channel. *Nature* **2006**,*443*, 230-233.

[50] Skryma R; Mariot P; Bourhis XL; Coppenolle FV; Shuba Y; Vanden Abeele F; Legrand G; Humez S; Boilly B; Prevarskaya N. Store depletion and store-operated Ca2+ current in human prostate cancer LNCaP cells: involvement in apoptosis. *J Physiol* **2000**,*527 Pt 1*, 71-83.

Figure legends

Fig. (1). Expression of TRPC channels in human ovarian cancer cells. A. Detection of TRPC mRNAs by RT-PCR using the primer set for TRPC1 (P3), TRPC3 (P4), TRPC4 (P5), TRPC5, TRPC6 (P3) and TRPC7 (see supplementary Table 1). The β-actin was used as positive control, and the reverse transcript step omitting the reverse transcriptase (no RT) was set as negative control. **B**. TRPC5 and TRPC7 were undetectable in (**A**), but positive if the plasmid TRPC5 and TRPC7 cDNAs were used as positive control. **C**. Western blotting detection of TRPC proteins using anti-TRPC1 (T1E3), anti-TRPC3, anti-TRPC4 (T45E3) and anti-TRPC6 (T367E3 (i) and anti-TRPC6 targeting to N-terminal (ii)) antibodies. No band was detected by anti-TRPC5 antibody (T5E3) in SKOV3, but positive for the rat brain lysate. Two bands were detected by anti-TRPC1 (T1E3) and competed by antigenic peptide.

Fig. (2). Detection of TRPC spliced variants in human ovarian cancer SKOV-3 cells. A. RT-PCR products of TRPC1 were amplified by specific primer set labelled as P1 to P5. Two products were amplified using primer set P1 with a size of 403 bp (TRPC1α) and 301 bp (TRPC1β). A small product with exon 9 deletion ($C1^{E9del}$) was identified using primer set P4 (405 bp for $C1^{E9del}$, and 549 bp for TRPC1α/β isoforms). The $C1^{E9del}$ was also detected using primer set P3 (423 bp for α/β isoforms; 279 bp for $C1^{E9del}$). No other splicing region was detected using primer set P2, P5 and the primer combinations amplifying exon 1-6 and exon 11-13. **B**. The TRPC3 spliced variant with an extended N-terminus was detected using primer set P0 (1221 bp). Single PCR product was found using primer set P1, P3 and P4, or P2 and the primers amplifying exon 8 to exon 12 (not shown). **C**. TRPC4 isoforms were detected by primer set P1 and P4. The ζ-isoform with exon 3 deletion ($C4^{E3del}$) amplified by set P2 (not shown) and ε-isoform amplified by isoform-specific primer were negative The γ-isoform with exon 8 deletion ($C4^{E8del}$) was detected by primer set P3, and P6 (not shown). Using primer set P7, both α-isoform (956 bp) and β-isoforms (704 bp) were detected. **D**. Two TRPC6 spliced isoforms were detected using primer set P1. Single band of TRPC6 with an expected size was detected by primer set P2 (551 bp) and P3 (476 bp). PCR products were confirmed by direct sequencing.

Fig. (3). Ovarian cancer cell proliferation was inhibited by store-operated channel blockers. A. SKOV3 were incubated with different concentrations of 2-APB for 24 h. The cell proliferation was monitored by WST-1 assay and the absorbance was measured at a wavelength of 450 nm with a reference at 600 nm. **B**. SKOV3 treated with carbenoxolone for 24 h. **C**. SKOV3 cells were incubated with carbenoxolone and 2-APB for 24 h. **D**. Effect of SKF-96365 on SKOV with a IC_{50} of 14.5 μM after 24 hour incubation. **E**. Effect of Gd^{3+}. **F**. Incubation with trypsin (0.1-10 nM). Each experiment had 8 well repeats and the data were from ≥ two independent experiments. *** $P<0.001$.

Fig. (4). Role of TRPC channels in the ovarian cancer growth. A. SKOV3 cells were incubated with functional antibodies (1:500 dilution for anti-TRPC1 (T1E3); 1:250 dilutions for anti-TRPC4 (T45E3), anti-TRPC5 (T5E3) and anti-TRPC6 (T367E3) for 24 hours and the cell proliferation was measured by WST-1 assay. n =16 for each group. **B**. SKOV3 cells were transfected with TRPC siRNAs (100 nM siRNA for each group) using Lipofectamine 2000. Cell proliferation was measured with WST-1 assay after 48 h transfection. The sham

transfection (control), pool siRNA and scramble siRNA were negative control. Bcl-2 siRNA was used as positive control. *n* =16 for each group. **C**. Ovarian cancer colony formation assay. The SKOV3 cells over-expressing with plasmid TRPC cDNAs (indicated) or vector and the cancer colonies were stained with crystal violet. **D**. Mean ± SE data showed the large (>2 mm^2) colony number. Triplicate wells were used for each group. Results were reproducible in more than three independent experiments. **E**. Examples of ovarian cancer colonies grown in soft agar and stained with crystal violet. The SKOV3 cells over-expressing with plasmid TRPC cDNAs (indicated) or vector. **F**. Mean ± SE data showed the number of large colony with a diameter >100 μm. Triplicate wells were used for each group. ** P<0.01, *** P<0.001.

Fig. (5). Cell cycle arrested by TRPC channel blocker SKF-96365 and TRPC siRNAs in ovarian cancer cells. A. The representative FACS histogram for vehicle (DMSO) and SKF-96365 (10 μM), and the mean ± SE data from three independent experiments. B. SKOV3 cells transfected with scramble siRNA (siScramble) and TRPC siRNA (siTRPC1, siTRPC4, siTRPC3, and siTRPC6) for 72 hours. The percentage of propidium iodide -labelled cells at different cell cycle stage was determined by FACS analysis. The mean ± SE data were from three independent experiments. * P<0.05, ** P<0.01, *** P<0.001 comparing with the vehicle group or the scramble siRNA transfected group.

Fig. (6). TRPC expression detected in human ovarian adenocarcinoma

The mRNA was detected by RT-PCR. The PCR amplicons for TRPC1 (i: primer P1; ii: primer P3), TRPC3, TRPC4 and TRPC6 were shown in (**A**). Five cancer samples from patients with undifferentiated ovarian serous papillary adenocarcinoma, and five normal samples were run in parallel. The GAPDH was used as control. **B**. The band density was quantified by a gel documentation software (VisionWorks LS6.3). The relative expression of TRPC/GAPDH was given. * P<0.05, *** P<0.001.

Fig. (7). Distribution of TRPC isoforms in human ovarian adenocarcinoma tissues and cells and the dependence of cell differentiation. A. Human ovarian adenocarcinoma tissue sections were stained with anti-TRPC1 (T1E3), anti-TRPC4 (T45E3), anti-TRPC3 (Alomone lab) and anti-TRPC6 (i:T367E3; ii:TRPC6 antibody from Alomone lab) using VECTASTAIN ABC Systems. The positive staining was shown as brown colour, and the nuclei were counter-stained by hematoxylin. The preimmue serum was used as control. Scale bar is 100 μm**. B.** Mean data for the staining intensity of the ovarian cancer. The *n* number is 15 microscopy fields for the quantification of the undifferentiated ovarian cancer from three patients, and *n* = 12 for the well differentiated ovarian tumour group from three patients. **C.** TRPC expression enhanced by all-*trans* retinoic acid (atRA). The mRNA was detected by real-time PCR. The GAPDH was used as a housekeeping gene for relative quantification. The $2^{(-\Delta\Delta Ct)}$ method was used for calculation. SKOV3 cells were treated with or without 1 μM atRA for 5 days. The culture media were refreshed every 24 hours. **D**. (i): SKOV3 cells stained with anti-TRPC1 (T1E3), anti-TRPC3, anti-TRPC4 (T45E3) and anti-TRPC6 antibodies at a dilution of 1:500 and the secondary anti-rabbit antibody conjugated with FITC (green). Same dilution of preimmune serum or no primary antibody was used as control. The nuclei were stained by 4',6-diamidino-2-phenylindole (DAPI, blue). Scale bar is 25 μm. (ii): Distribution of TRPC isoforms in the transfected HEK-293 T-REx cells. The TRPC1, $TRPC1^{E9del}$ and TRPC6 cDNAs were tagged with CFP (blue), TRPC3 tagged with mCherry (Red), and TRPC4 (α, β and ε isoforms) tagged with EYFP. ** P<0.01, *** P<0.001.

Supplementary methods

Fluorescence activated cell sorting (FACS). The cell surface binding of the E3-targeting antibodies were examined by FACS using TRPC-transfected HEK-293 cells. Briefly, the HEK-293 cells transfected with TRPC genes were dissociated from a flask and transferred to a 5-ml FACS tube with PBS. The cells were centrifuged at 300 g for 5 min at 4˚C and the cell pellet was resuspended in PBS. The anti-TRPC antibodies were added (1:500) into the tube and cells were incubated at room temperature for 15 min and 1 hour at 4˚C. The cells were washed by PBS three times via centrifugation and resuspension. The sheep anti-rabbit secondary antibody conjugated with FITC was added and incubated for 1 hour at 4˚C. The cells were washed again with PBS for three times and harvested for FACS assay.

Electrophysiological recordings. Whole-cell clamp was performed at room temperature (23-26°C). Briefly, signal was amplified with an Axopatch 200B patch clamp amplifier and controlled with pClamp software version 10. A 1-s ramp voltage protocol from –100 mV to +100 mV was applied at a frequency of 0.2 Hz from a holding potential of 0 mV. Signals were sampled at 10 kHz and filtered at 1 kHz. The glass microelectrode with a resistance of 3-5 MΩ was used. The 200 nM Ca^{2+} buffered pipette solution contained 115 CsCl, 10 EGTA, 2 $MgCl_2$, 10 HEPES, and 5.7 $CaCl_2$ in mM, pH was adjusted to 7.2 with CsOH and osmolarity was adjusted to ~290 mOsm with mannitol, and the calculated free Ca^{2+} was 200 nM using EQCAL (Biosoft, Cambridge, UK). The standard bath solution contained (mM) : 130 NaCl, 5 KCl, 8 D-glucose, 10 HEPES, 1.2 $MgCl_2$ and 1.5 $CaCl_2$. The pH was adjusted to 7.4 with NaOH.

Fig. S1. Specific binding of functional anti-TRPC Antibodies. The specific binding of E3-targeting (FACS) using HEK293 cells transiently transfected with TRPC1, TRPC4, TRPC5 and TRPC6 plasmid cDNA. Control: HEK-293 cells with mock transfection. (**B**). The antibodies with 1:250-500 dilution were used for FACS.

Fig. S2. RT-PCR detection of TRPC1-7 in mouse brain. TRPC1-7 mRNAs were detected by RT-PCR using mouse brain total RNA and the primer set in the supplementary Table 1. The procedure was similar to the experiment on SKOV3 (see Fig.1A). TRPC1 (423 bp), TRPC3 (318 bp), TRPC4 (415 bp), TRPC5 (489 bp), TRPC6 (551 bp) and TRPC7 (398 bp) were detected.

Fig. S3. Sequence alignment of human TRPC4 isoforms. The γ-isoform has exon 8 deletion, and ε-isoform has a 5 amino acids insert between exon 8 and exon 9. The zeta isoform has exon 3 deletion (not shown). The gene accession numbers are: NM_016179 (alpha); NM_001135955 (beta); NM_001135956 (gamma); NM_001135957 (delta); NM_003306 (epsilon); NM_001135958 (Zeta).

Fig. S4. Whole-cell current of TRPC isoforms overexpressing in HEK293 T-REx cells. A. HEK293 T-REx cells inducibly transfected with TRPC3 tagged with mCherry**. B.** current-voltage **(**IV) curve for TRPC3. **C.** HEK293 T-REx cells inducibly transfected with TRPC4 tagged with EYFP. **D.** The *IV* curve for TRPC4. **E.** HEK293 T-REx cells inducibly transfected with TRPC6 tagged with CFP. **F.** The *IV* curve for TRPC6. 2-APB (100 μM) and trypsin 0.1 nM were used in the experiments.

Fig. S5. Functional properties of TRPC4 splicing isoforms. Whole-cell current of TRPC4 isoforms inducibly overexpressing in HEK293 T-REx cells. **A.** HEK293 T-REx cells transfected with TRPC4α tagged with EYFP**. B.** Current-voltage **(***IV*) curve for TRPC4α. **C.** HEK293 T-REx cells transfected with TRPC4β tagged with EYFP. **D.** The *IV* curve for TRPC4β. **E.** HEK293 T-REx cells transfected with TRPC4ε tagged with EYFP. **F.** The *IV* curve for TRPC4ε. Gd^{3+} (100 μM) and 2-APB (100 μM) were used in all the experiments.

Fig. S6. Impermeable staining of SKOV3 with anti-TRPC antibodies. The anti-TRPC1 (T1E3), anti-TRPC4 (T45E3) and anti-TRPC6 (T367E3) were used. The TRPC protein staining shown as green, and the nuclei were stained with DAPI (blue).

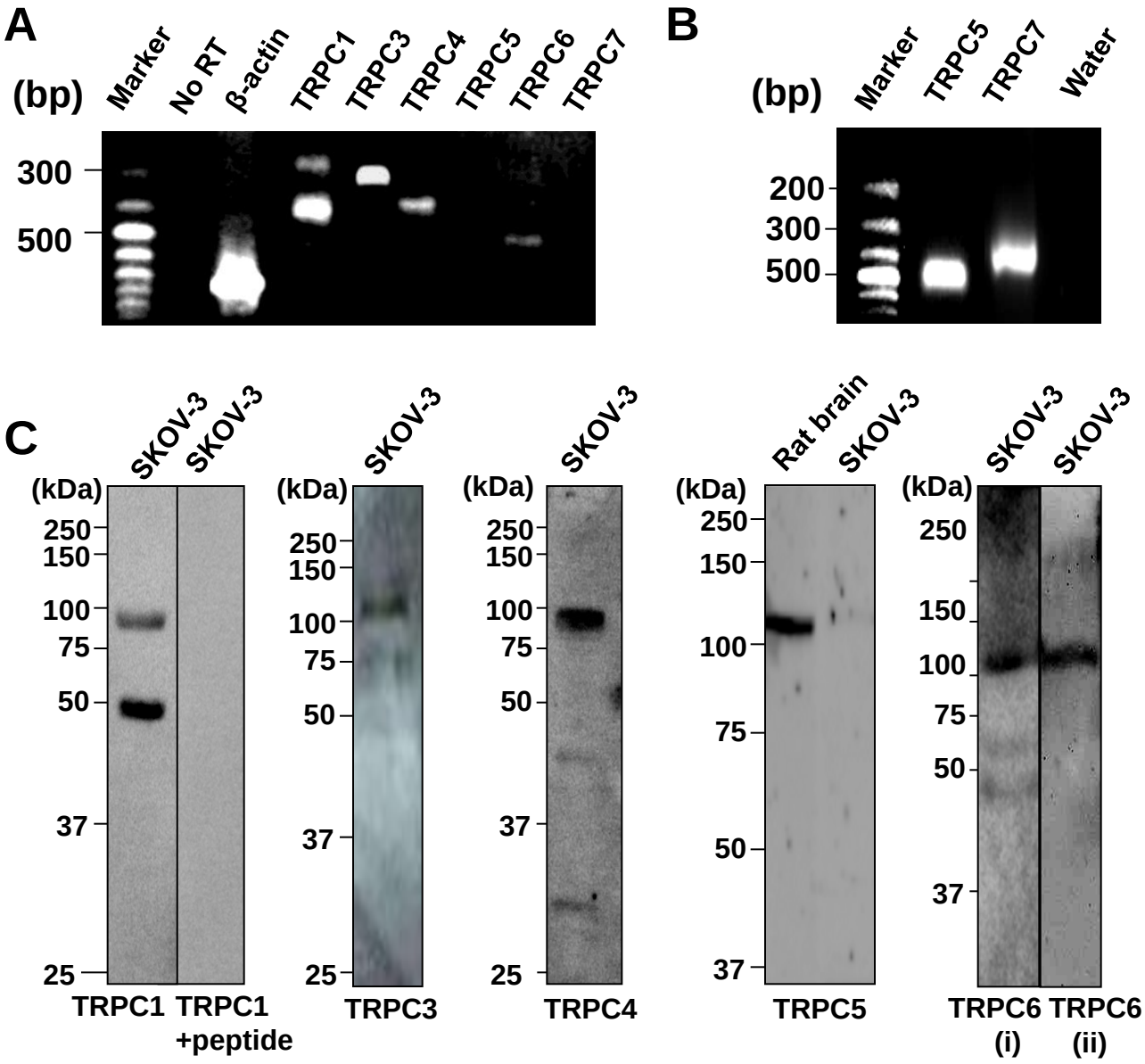
A
(bp)
Marker
No RT
β-actin
TRPC1
TRPC3
TRPC4
TRPC5
TRPC6
TRPC7
300
500
B
(bp)
Marker
TRPC5
TRPC7
Water
200
300
500
C
SKOV-3
SKOV-3
(kDa)
250
150
100
75
50
37
25
TRPC1
TRPC1 +peptide
SKOV-3
TRPC3
SKOV-3
TRPC4
Rat brain
SKOV-3
TRPC5
SKOV-3
SKOV-3
TRPC6 (i)
TRPC6 (ii)

Figure 1

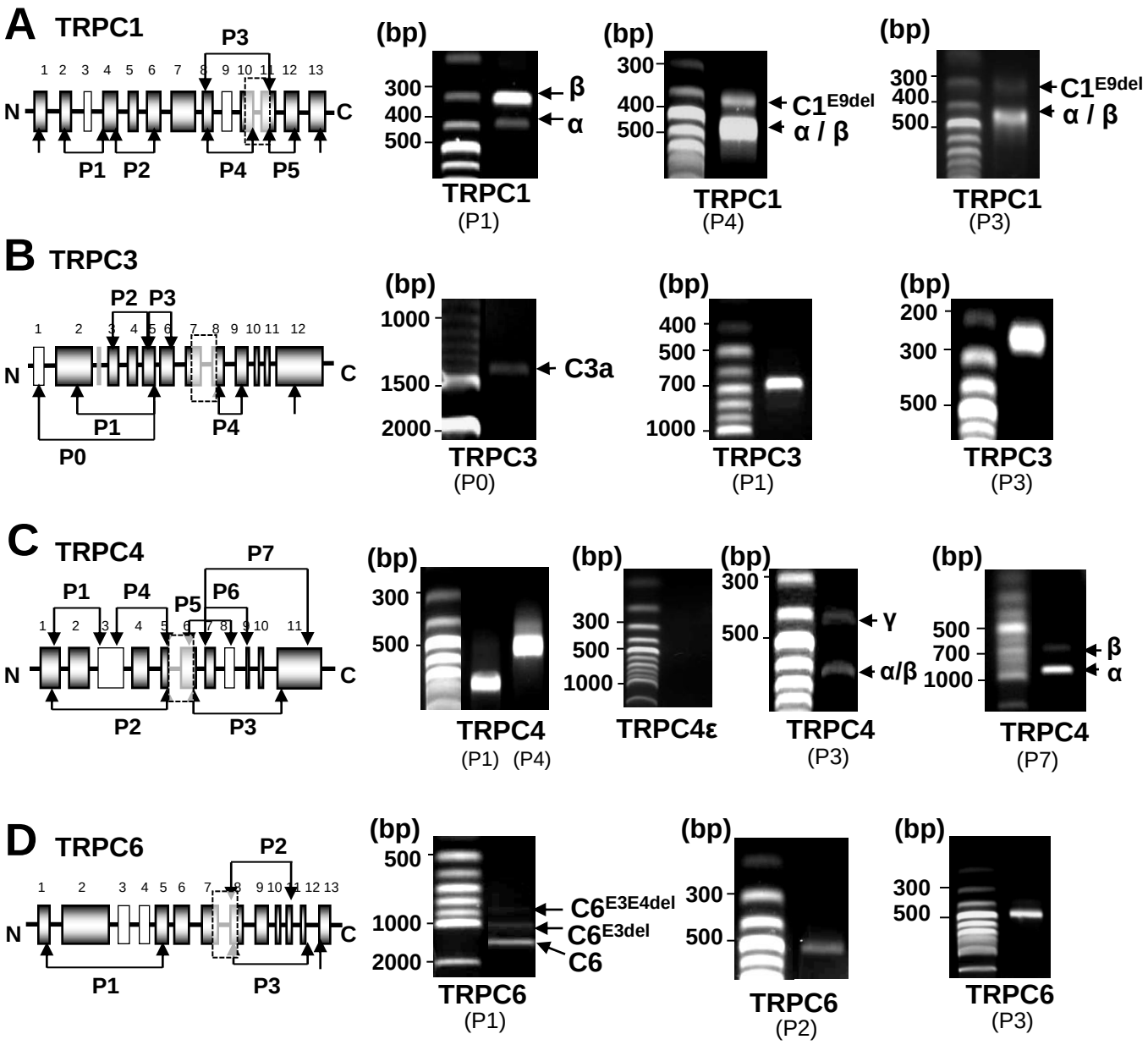
A TRPC1
P3
1 2 3 4 5 6 7 8 9 10 11 12 13
N
C
P1 P2 P4 P5
(bp)
300
400
500
β
α
TRPC1
(P1)
(bp)
300
400
500
C1E9del
α / β
TRPC1
(P4)
(bp)
300
400
500
C1E9del
α / β
TRPC1
(P3)
B TRPC3
P2 P3
1 2 3 4 5 6 7 8 9 10 11 12
N
C
P1
P4
P0
(bp)
1000
1500
2000
C3a
TRPC3
(P0)
(bp)
400
500
700
1000
TRPC3
(P1)
(bp)
200
300
500
TRPC3
(P3)
C TRPC4
P7
P1 P4 P5 P6
1 2 3 4 5 6 7 8 9 10 11
N
C
P2 P3
(bp)
300
500
TRPC4
(P1) (P4)
(bp)
300
500
1000
TRPC4ε
(bp)
300
500
γ
α/β
TRPC4
(P3)
(bp)
500
700
1000
β
α
TRPC4
(P7)
D TRPC6
P2
1 2 3 4 5 6 7 8 9 10 11 12 13
N
C
P1
P3
(bp)
500
1000
2000
C6E3E4del
C6E3del
C6
TRPC6
(P1)
(bp)
300
500
TRPC6
(P2)
(bp)
300
500
TRPC6
(P3)

Figure 2

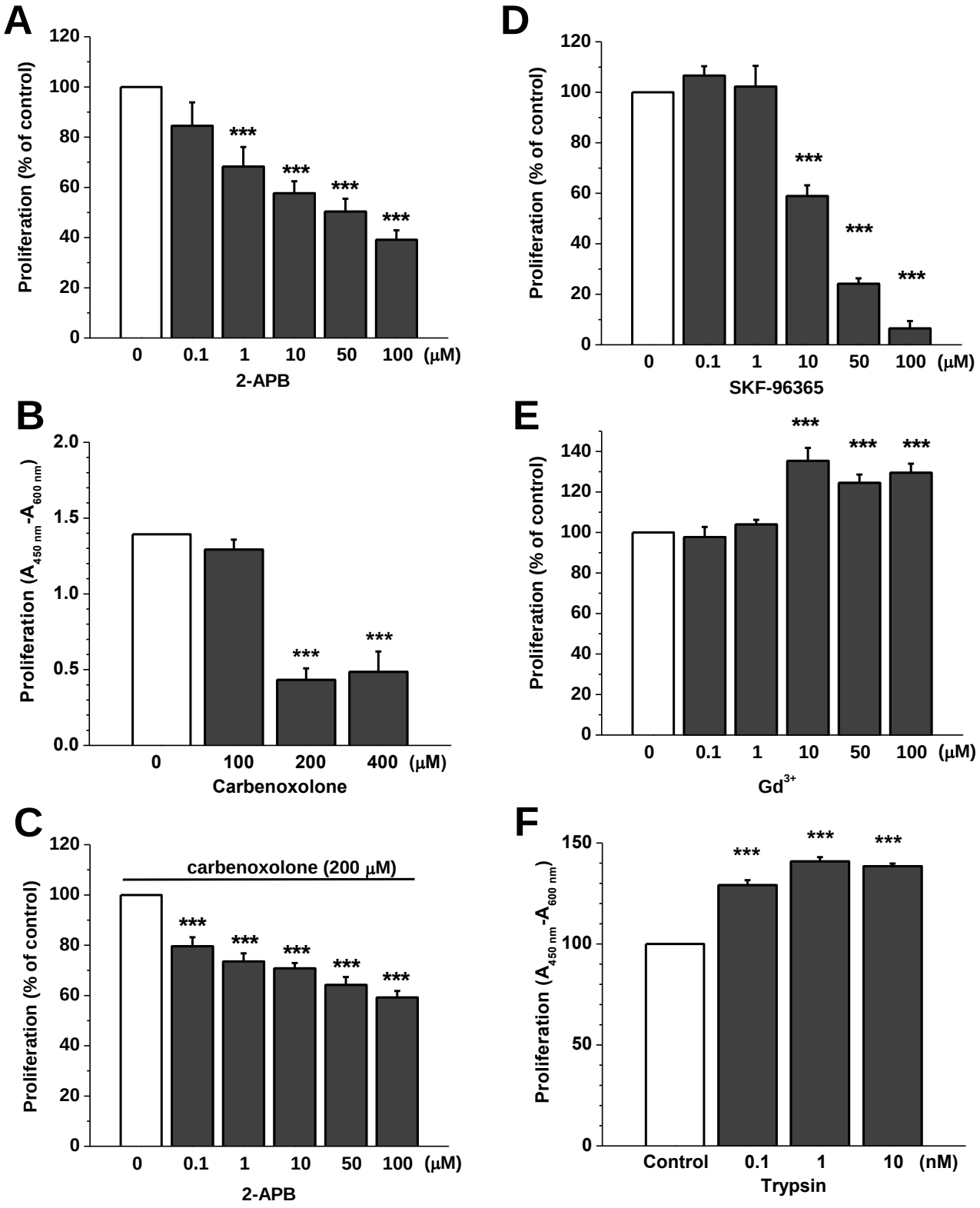
A
Proliferation (% of control)
120
100
80
60
40
20
0
***
***
***
***
0
0.1
1
10
50
100
(μM)
2-APB
D
Proliferation (% of control)
120
100
80
60
40
20
0
***
***
***
0
0.1
1
10
50
100
(μM)
SKF-96365
B
Proliferation ($A_{450\ nm}$-$A_{600\ nm}$)
2.0
1.5
1.0
0.5
0.0
***
***
0
100
200
400
(μM)
Carbenoxolone
E
Proliferation (% of control)
140
120
100
80
60
40
20
0
***
***
***
0
0.1
1
10
50
100
(μM)
Gd^{3+}
C
Proliferation (% of control)
120
100
80
60
40
20
0
carbenoxolone (200 μM)
***
***
***
***
***
0
0.1
1
10
50
100
(μM)
2-APB
F
Proliferation ($A_{450\ nm}$-$A_{600\ nm}$)
150
100
50
0
***
***
***
Control
0.1
1
10
(nM)
Trypsin

Figure 3

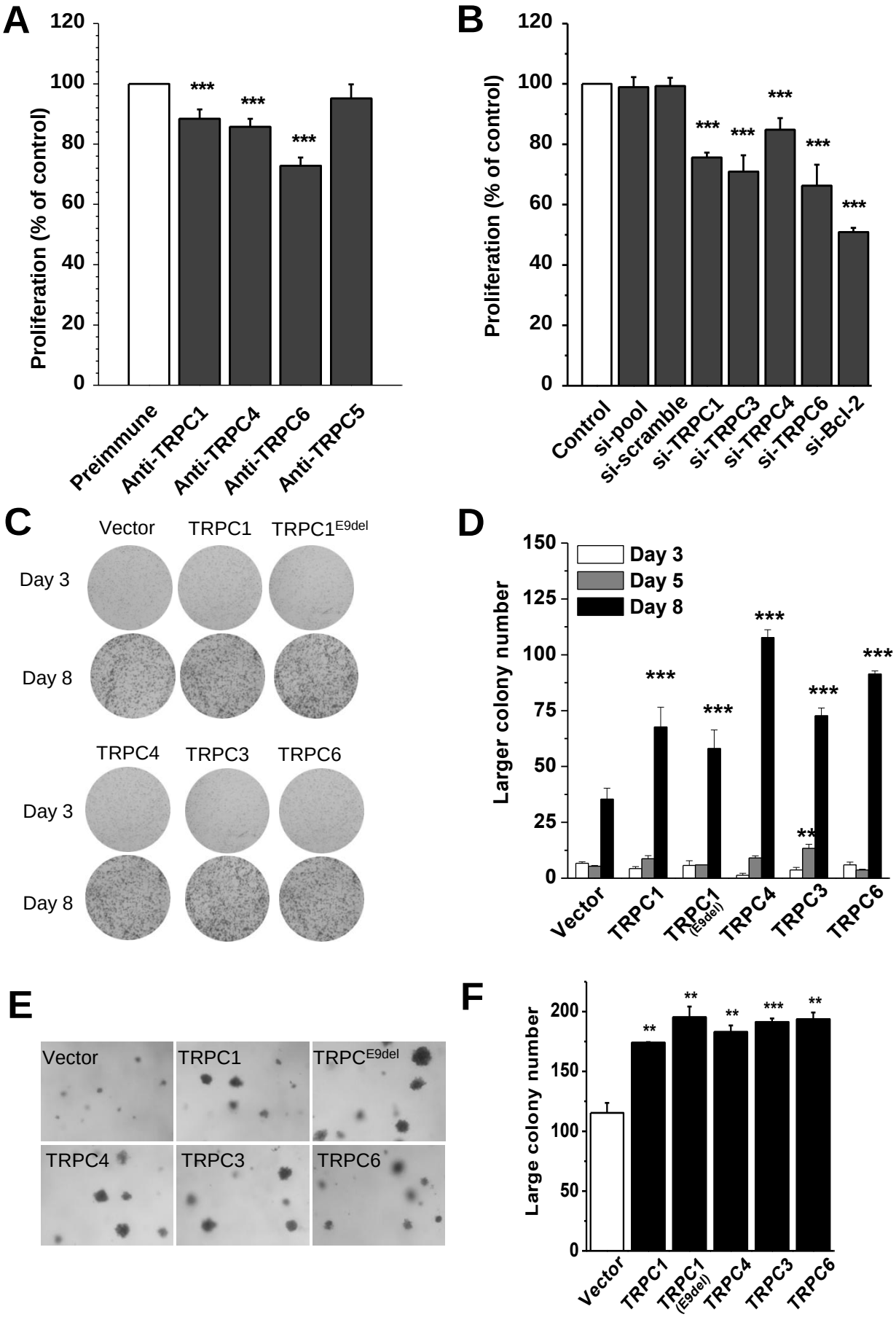
A
Proliferation (% of control)
120
100
80
60
40
20
0
***
***
***
Preimmune
Anti-TRPC1
Anti-TRPC4
Anti-TRPC6
Anti-TRPC5
B
Proliferation (% of control)
120
100
80
60
40
20
0
***
***
***
***
***
Control
si-pool
si-scramble
si-TRPC1
si-TRPC3
si-TRPC4
si-TRPC6
si-Bcl-2
C
Vector
TRPC1
TRPC1E9del
Day 3
Day 8
TRPC4
TRPC3
TRPC6
Day 3
Day 8
D
Larger colony number
150
125
100
75
50
25
0
Day 3
Day 5
Day 8
***
***
***
**
***
***
Vector
TRPC1
TRPC1 (E9del)
TRPC4
TRPC3
TRPC6
E
Vector
TRPC1
TRPCE9del
TRPC4
TRPC3
TRPC6
F
Large colony number
200
150
100
50
0
**
**
**
***
**
Vector
TRPC1
TRPC1 (E9del)
TRPC4
TRPC3
TRPC6

Figure 4

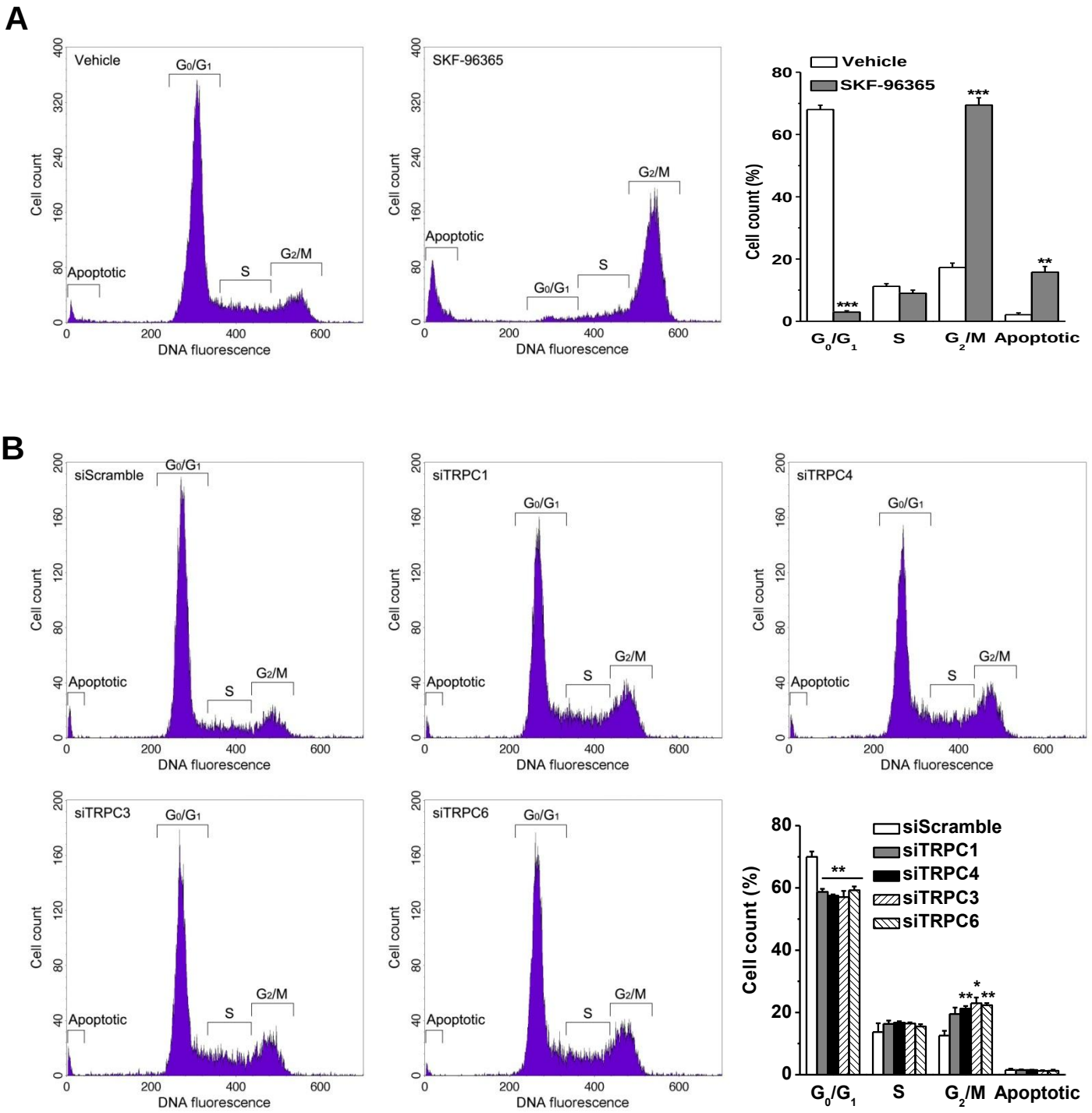
A
Vehicle
G0/G1
Apoptotic
S
G2/M
Cell count
DNA fluorescence
SKF-96365
Vehicle
Cell count (%)
***
**
G0/G1
S
G2/M
Apoptotic
B
siScramble
siTRPC1
siTRPC4
siTRPC3
siTRPC6
siScramble
siTRPC1
siTRPC4
siTRPC3
siTRPC6
*

Figure 5

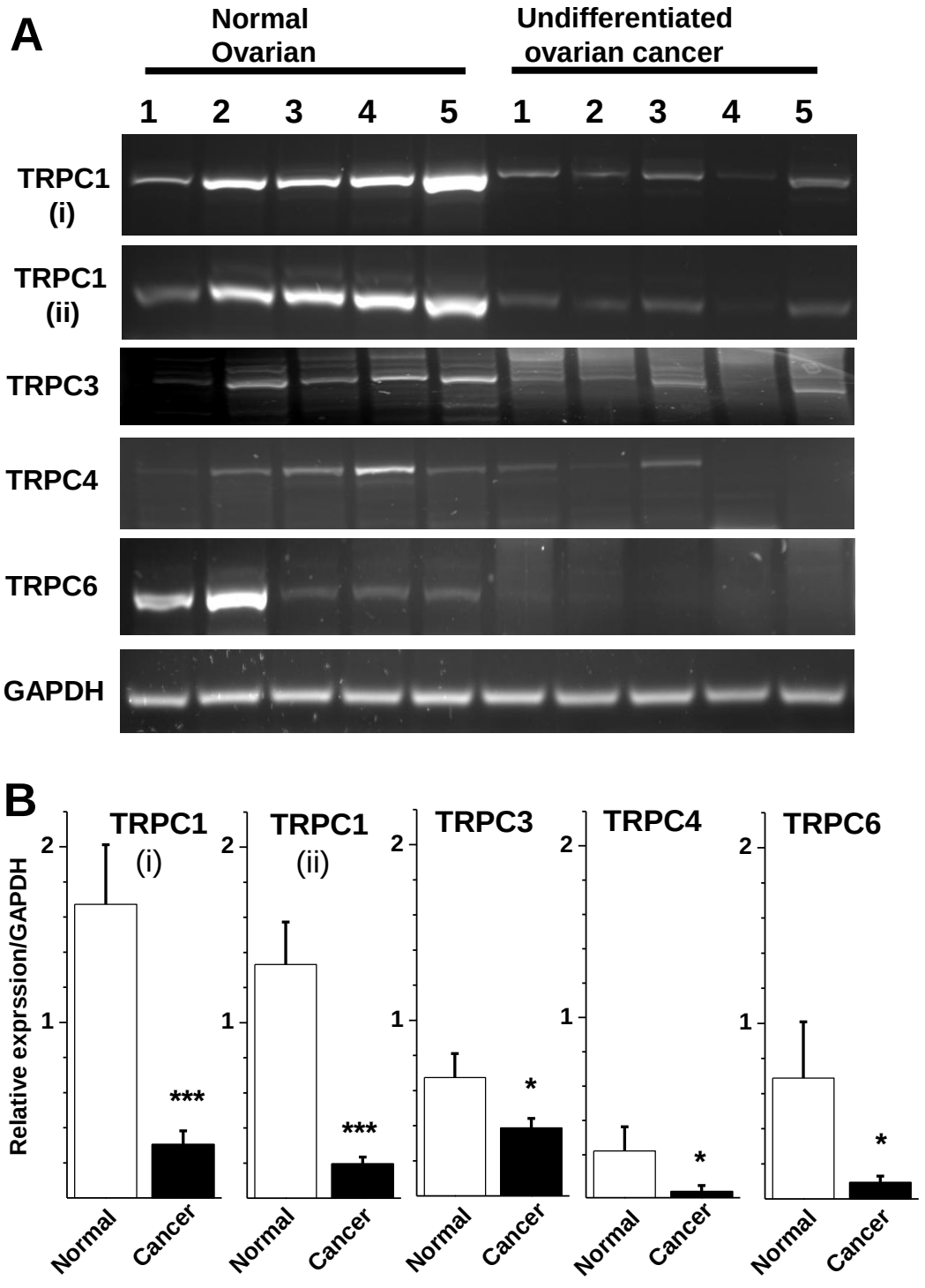
A
Normal Ovarian
Undifferentiated ovarian cancer
1 2 3 4 5 1 2 3 4 5
TRPC1 (i)
TRPC1 (ii)
TRPC3
TRPC4
TRPC6
GAPDH
B
Relative exprssion/GAPDH
TRPC1 (i)
TRPC1 (ii)
TRPC3
TRPC4
TRPC6
***
***
*
*
*
Normal
Cancer

Figure 6

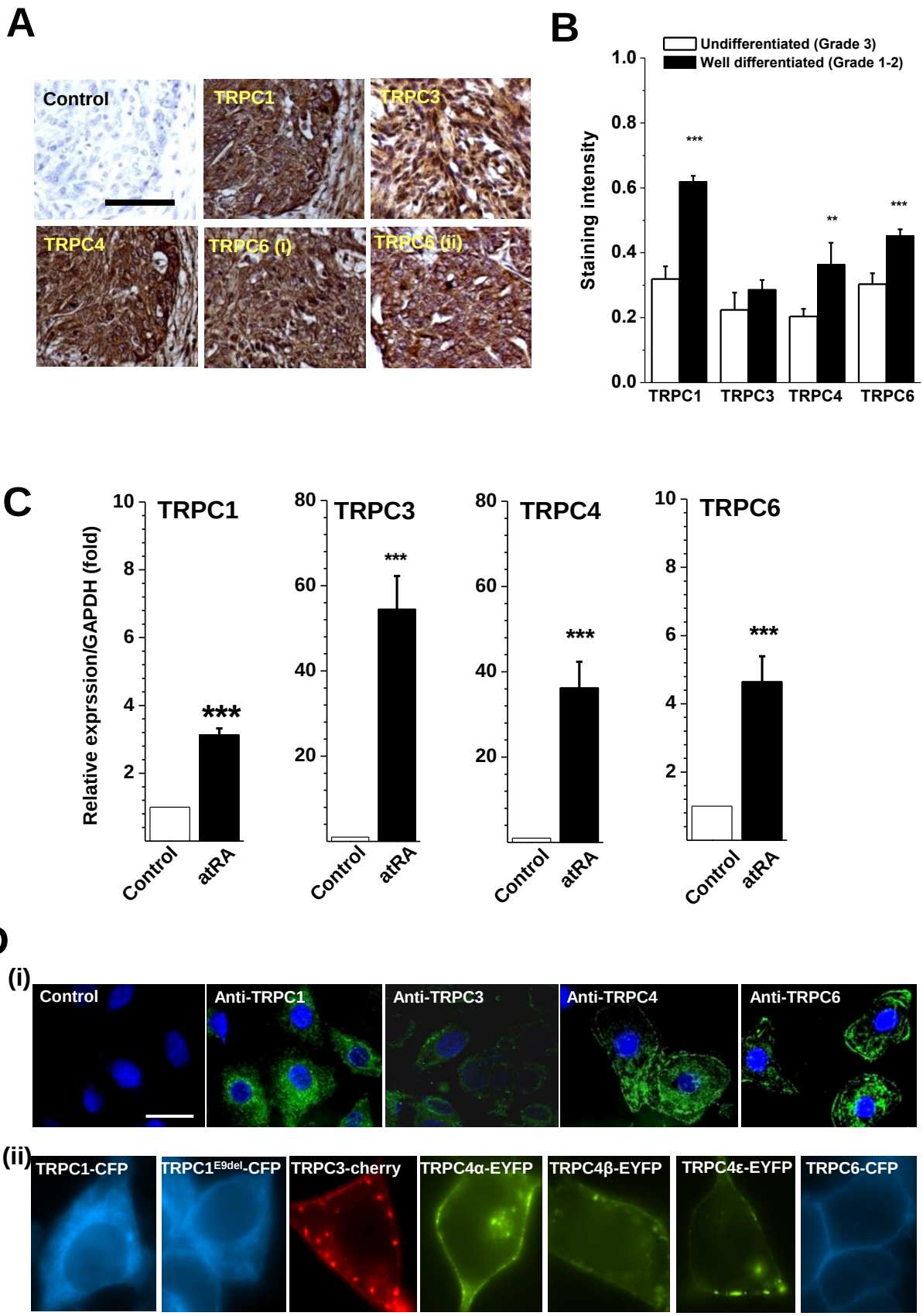
A
Control
TRPC1
TRPC3
TRPC4
TRPC6 (i)
TRPC6 (ii)
B
Undifferentiated (Grade 3)
Well differentiated (Grade 1-2)
Staining intensity
1.0
0.8
0.6
0.4
0.2
0.0
***
**
***
TRPC1
TRPC3
TRPC4
TRPC6
C
Relative exprssion/GAPDH (fold)
TRPC1
TRPC3
TRPC4
TRPC6
***
Control
atRA
D
(i)
Control
Anti-TRPC1
Anti-TRPC3
Anti-TRPC4
Anti-TRPC6
(ii)
TRPC1-CFP
TRPC1E9del-CFP
TRPC3-cherry
TRPC4α-EYFP
TRPC4β-EYFP
TRPC4ε-EYFP
TRPC6-CFP

Figure7

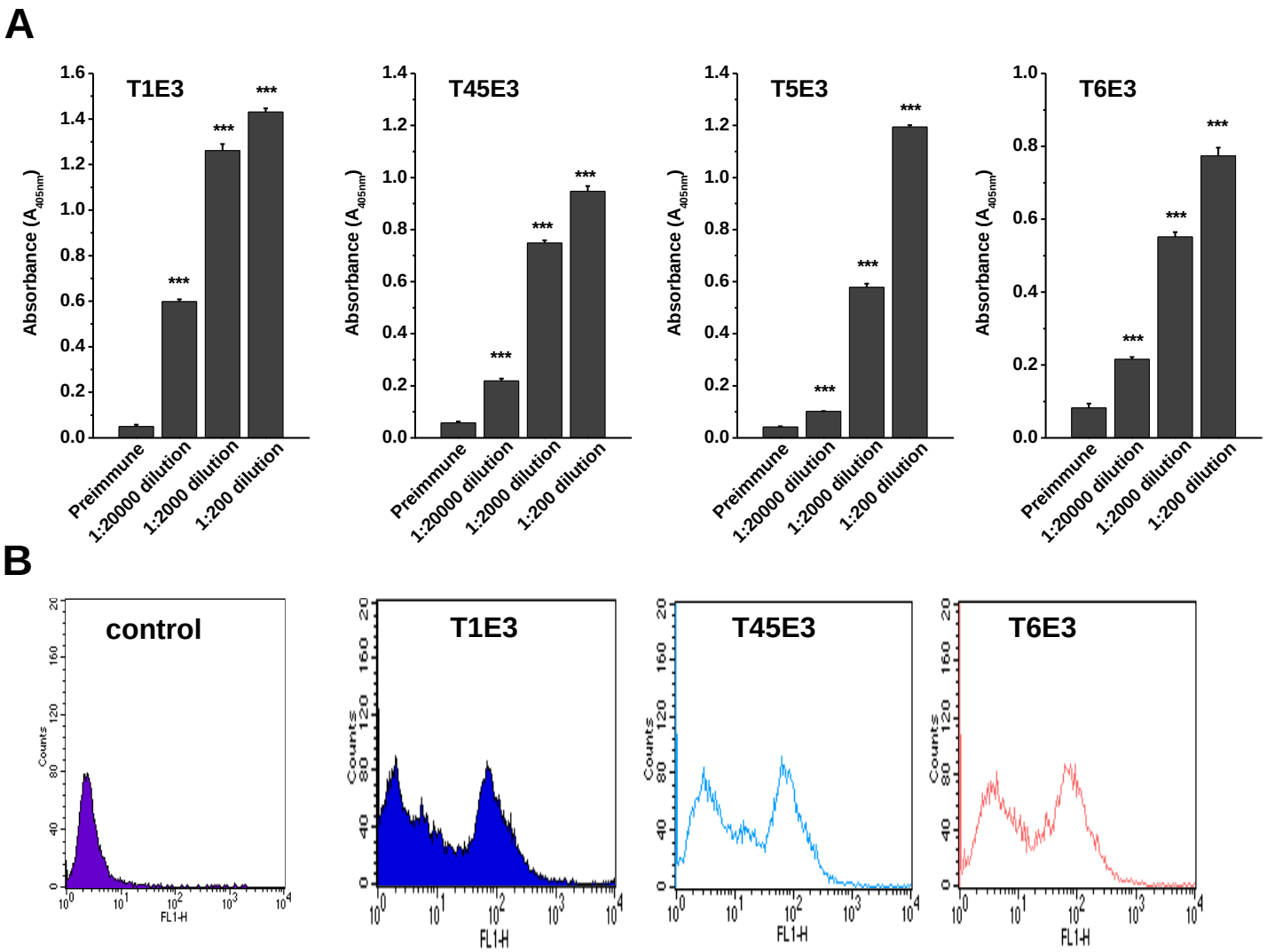
A
T1E3
T45E3
T5E3
T6E3
Absorbance (A405nm)
***
Preimmune
1:20000 dilution
1:2000 dilution
1:200 dilution
B
control
T1E3
T45E3
T6E3
Counts
FL1-H

Fig. S1

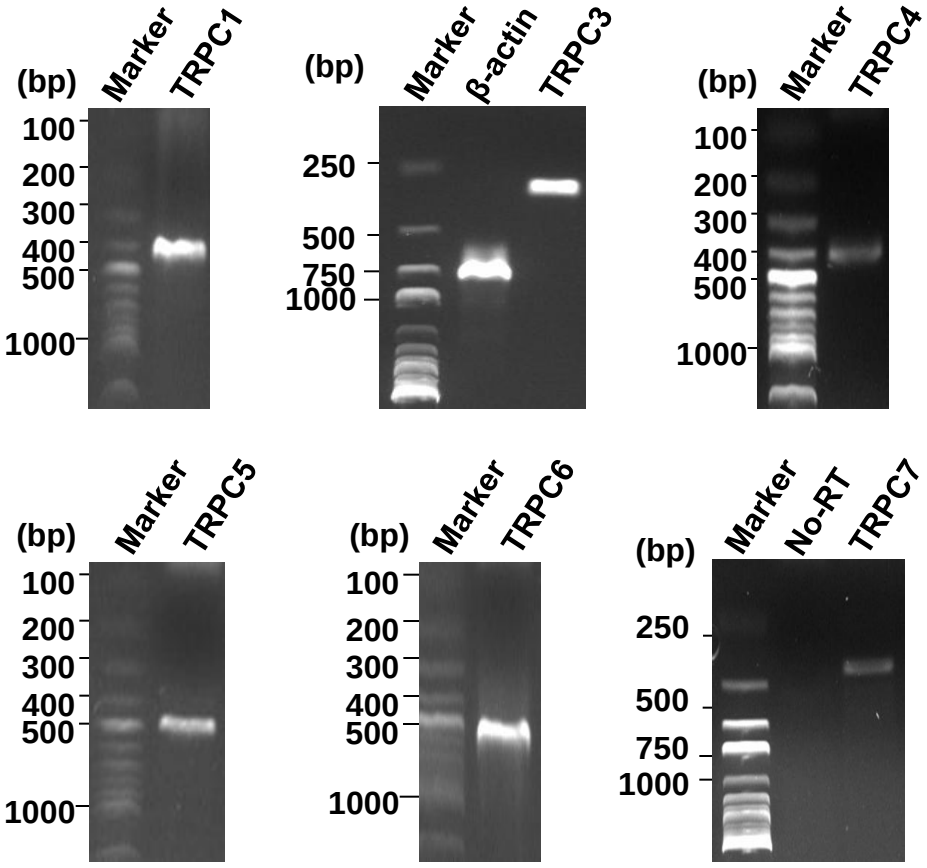
(bp)
Marker
TRPC1
100
200
300
400
500
1000
(bp)
Marker
β-actin
TRPC3
250
500
750
1000
(bp)
Marker
TRPC4
100
200
300
400
500
1000
(bp)
Marker
TRPC5
100
200
300
400
500
1000
(bp)
Marker
TRPC6
100
200
300
400
500
1000
(bp)
Marker
No-RT
TRPC7
250
500
750
1000

Fig. S2

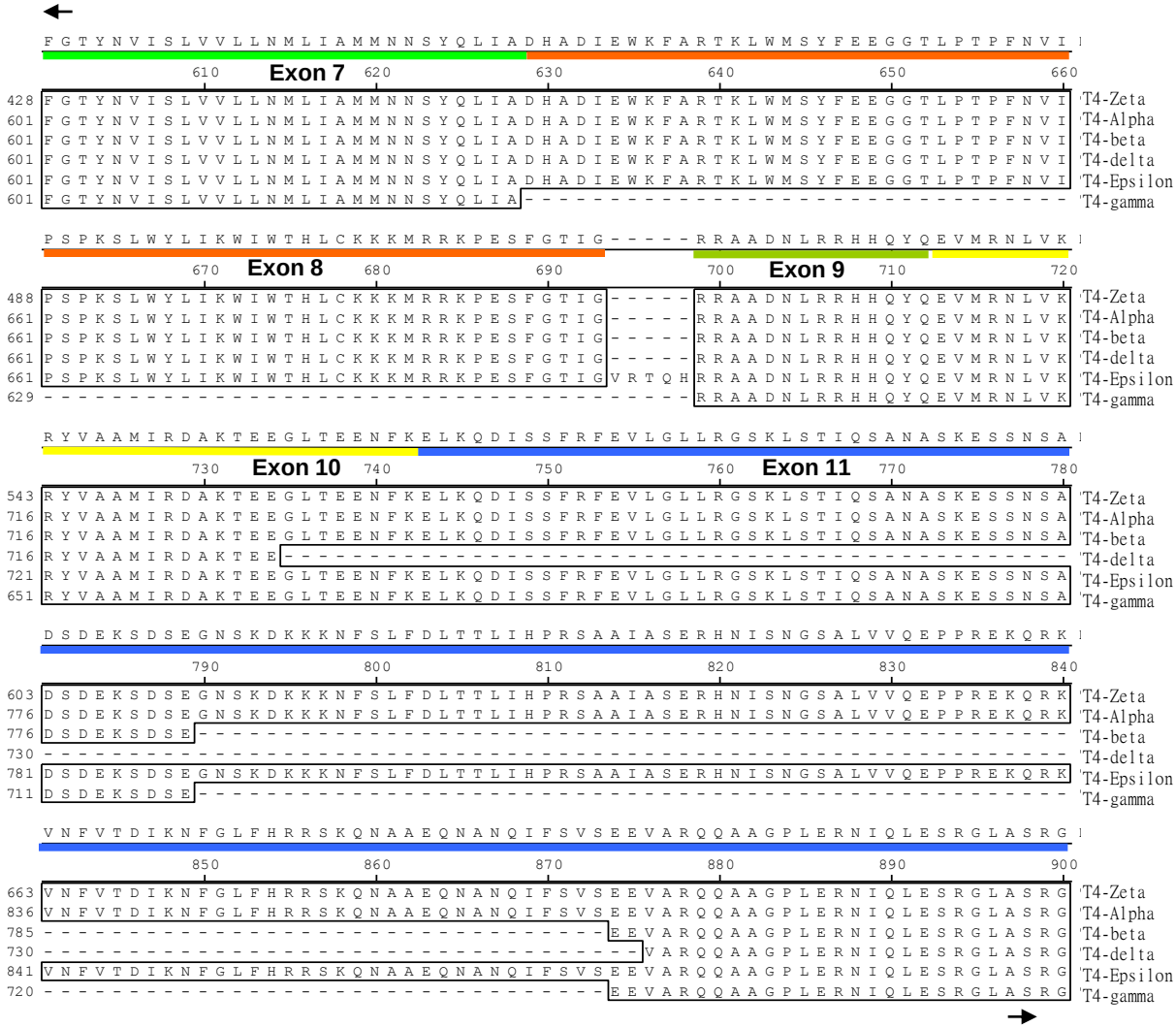
Exon 7
Exon 8
Exon 9
Exon 10
Exon 11
T4-Zeta
T4-Alpha
T4-beta
T4-delta
T4-Epsilon
T4-gamma

Fig. S3

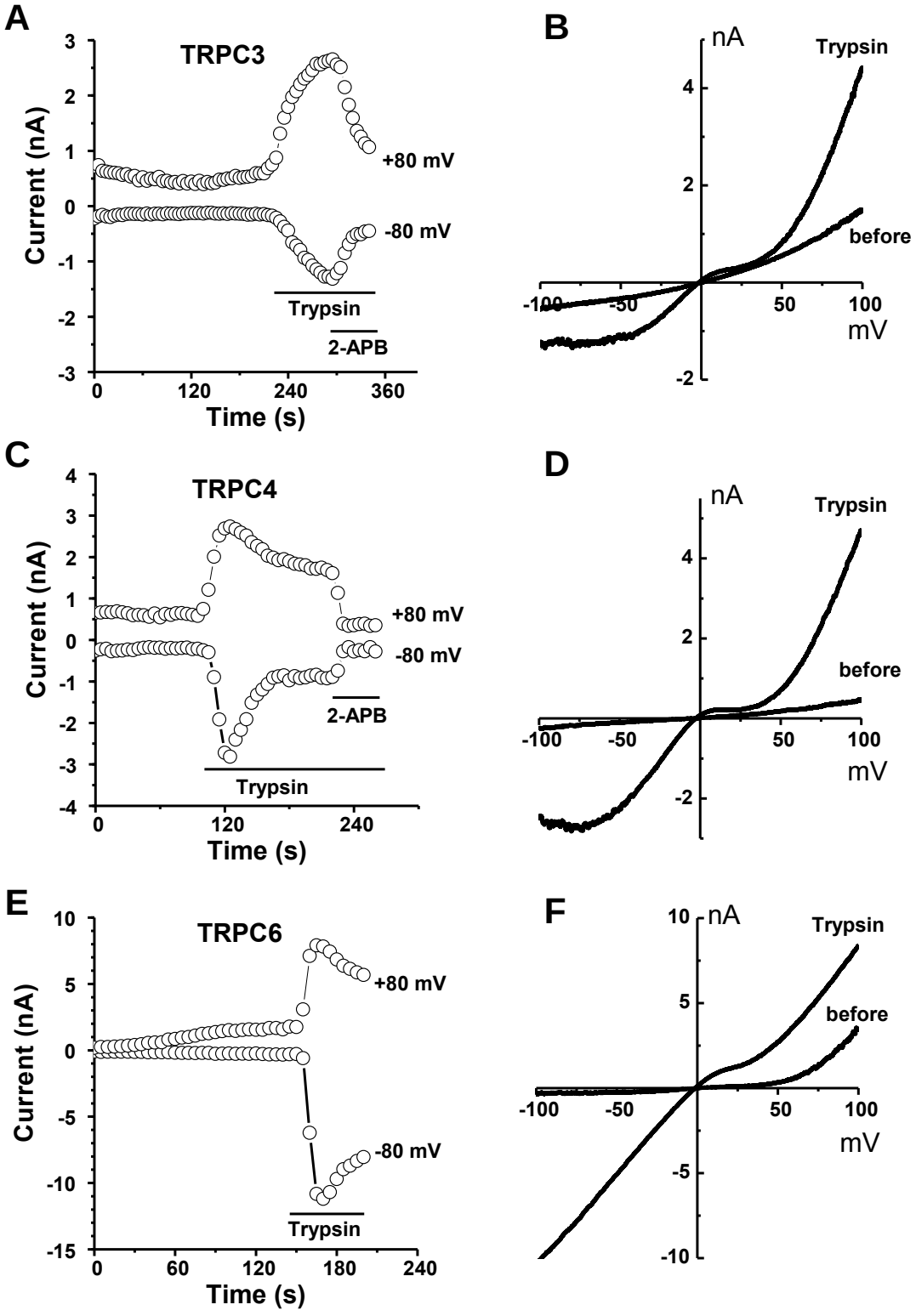
A
TRPC3
Current (nA)
Time (s)
+80 mV
-80 mV
Trypsin
2-APB
B
nA
Trypsin
before
mV
C
TRPC4
Current (nA)
Time (s)
+80 mV
-80 mV
2-APB
Trypsin
D
nA
Trypsin
before
mV
E
TRPC6
Current (nA)
Time (s)
+80 mV
-80 mV
Trypsin
F
nA
Trypsin
before
mV

Fig. S4

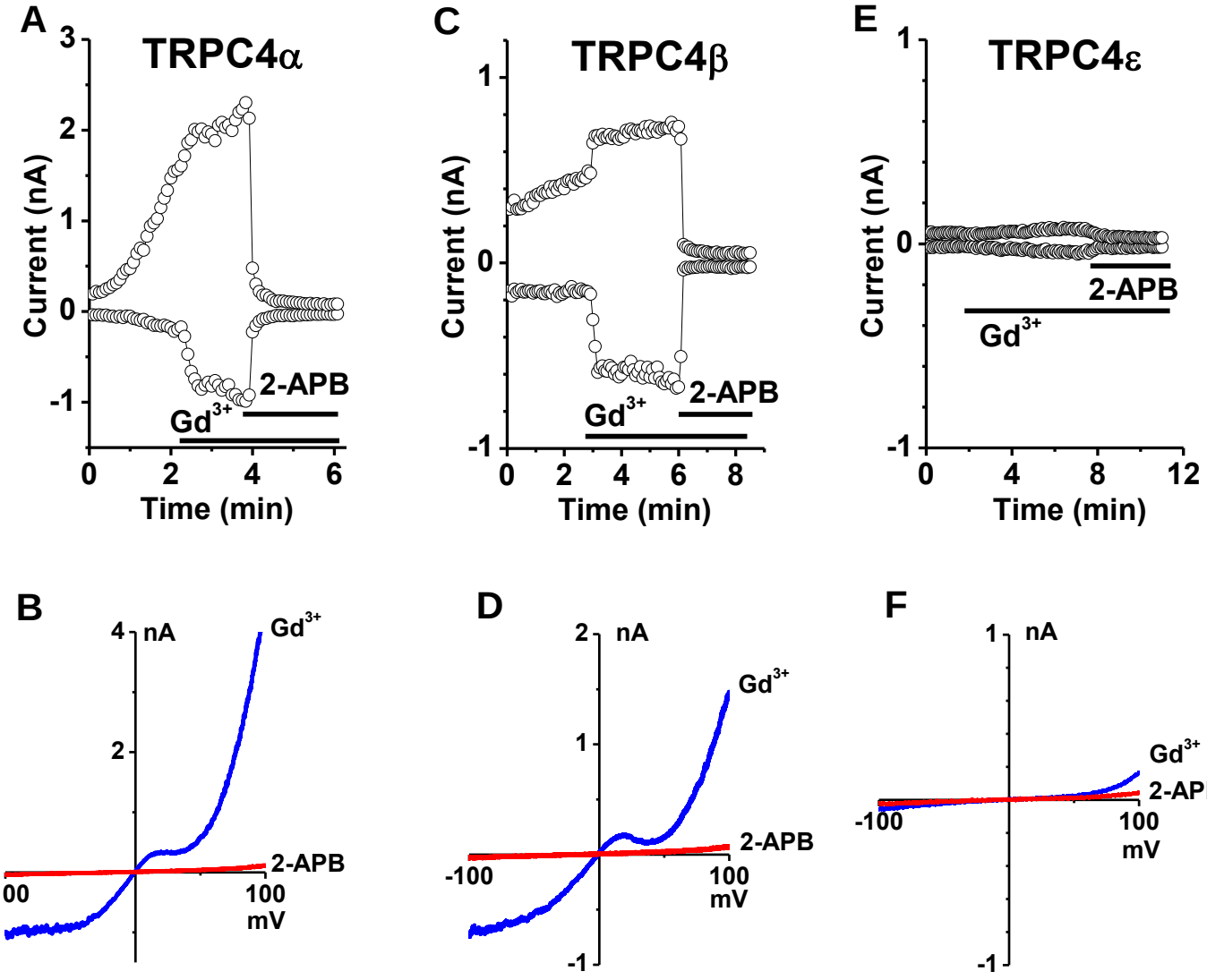
A
TRPC4α
Current (nA)
Time (min)
2-APB
Gd3+
C
TRPC4β
Current (nA)
Time (min)
2-APB
Gd3+
E
TRPC4ε
Current (nA)
Time (min)
2-APB
Gd3+
B
nA
Gd3+
2-APB
-100
100
mV
D
nA
Gd3+
2-APB
-100
100
mV
F
nA
Gd3+
2-APB
-100
100
mV

Fig. S5

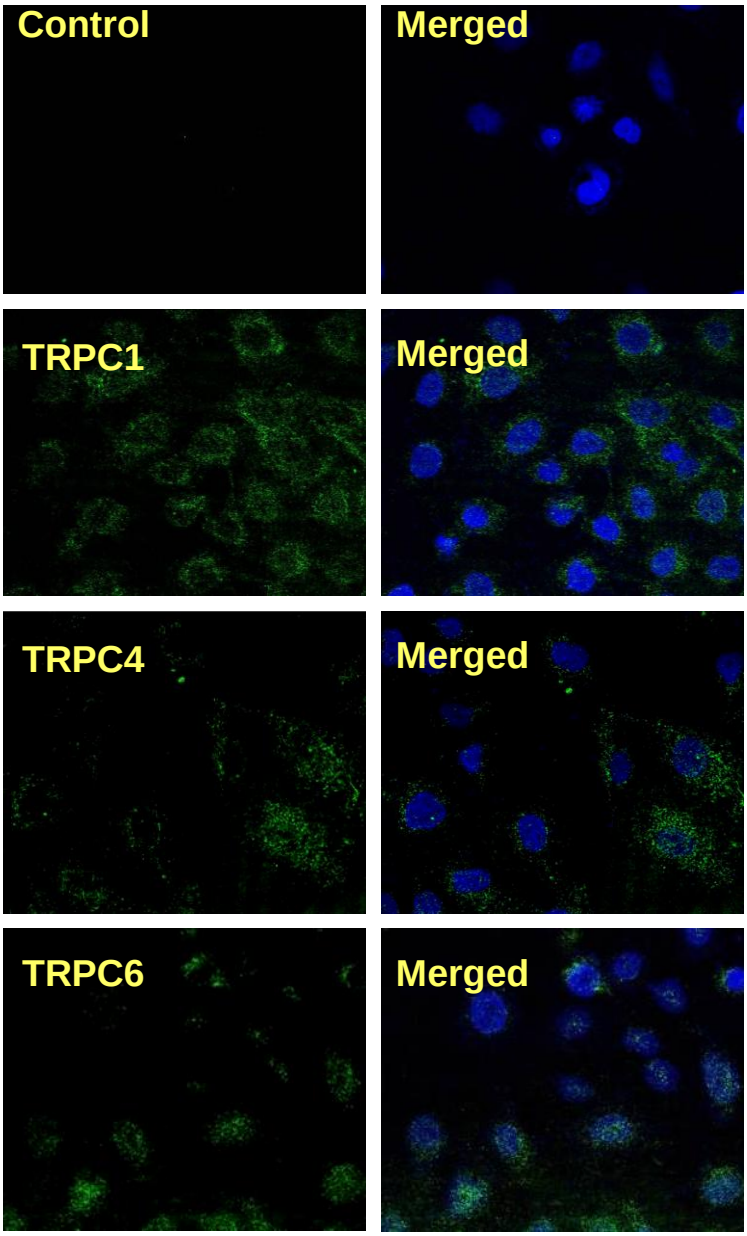

Fig. S6

Supplementary table 1. Primer sequences for RT-PCR

Gene name		Primers (5' to 3')	Location	Exon		Size (bp)
β-actin (NM_001101.3)	F	TTGTAACCAACTGGGACGATATG	313-326			759
	R	GATCTTGATCTTCATGGTGCTGG	1071-1049			
TRPC1 (NM_003304)	F	GGGAGGTGAAGGAGGAGAAT	249-268	E1		
	F	GATGTGCTTGGGAGAAATGC	377-396	E2	P1	402 (301)
	R	CAAGACGAAACCTGGAATGC	677-658	E4		
	F	TGCACCTGTCATTTTAGCTG	514-533	E4	P2	164
	R	CAAGACGAAACCTGGAATGC	677-658	E6		
	F	TGGTATGAAGGGTTGGAAGAC	1361-1381	E8	P3	423
	R	GGTATCATTGCTTTGCTGTTC	1783-1763	E10		
	R	AATGACAGCTCCCACAAAGG	1909-1890	E11	P4	549 (405)
	F	TGCTTACCAAACTGCTGGTG	1941-1960	E11	P5	243
	R	AACTGTTTTGCCGTTTGACC	2183-2164	E12		
	R	TGCACTAGGCAGCACATCA	2253-2235	E13		
TRPC3 (NM_001130698)	F	AACAAGCAAGGGTGACCTTC	103-122	E1	P0	1405
	F	AAGGGTGCCAGGATCGAG	837-854	E2	P1	671
	F	TGGAGATCTGGAATCAGCAG	1157-1176	E3	P2	351
	R	GAGGCATTGAACACAAGCAG	1507-1488	E5		
	F	GCAGCTCTTGACGATCTGGT	1277-1296	E4		238
	R	CCTGTCTGAGGCATTGAACA	1514-1495	E5		
	F	CTGGGTCTGCTTGTGTTCAA	1482-1501	E5	P3	248
	R	ATGGACAGCATCCCAAAGTC	1729-1710	E6		
	F	TGACTTCCGTTGTGCTCAAATATG	2185-2208	E8	P4	318
	R	CCTTCTGAAGTCTTCTCCTTCTGC	2502-2479	E9		
	R	TTCCTCAGTTGCTTGGCTCT	2777-2758	E12		
TRPC4 (NM_016179.2)	F	CTCCAGCTTCGATCGTTTTC	53-72	E1	P1	740
	R	TCTGAACTGGACACGCATTC	792-773	E3		
	F	CTCGGATCCCATCACTTCAG	163-182	E1	P2	1994 (734)
	R	TCCCATGATTCTCGTGGATT	2157- 2131	E6		
	F	TCTGCAGATATCTCTGGGAAGGATGC	1747-1772	E6	P5	415
	R	AAGCTTTGTTCGAGCAAATTTCCATTC	2161-2135	E8		
	F	GGATCAGACGAGAAGTTCCAG	1003-1023	E3	P4	519
	R	TAGTCCTGAAGTCCGCCATC	1521-1502	E5		
	F	CGAAAGGGTTAACCTGCAAA	1866-1885	E6	P3	623 (493)
	R	CAGGACTTCAAAGCGGAAAC	2488-2469	E11		
	F	CAATGTCATCTCTCTGGTTGTTC	2047-2069	E7	P6	309
	R	TGGTATTGGTGATGTCTTCTCAAG	2355-2332	E9		
	R	ATGCTGTGTTCTTACCCCT	2329-2311	Epsilon	P7	
	R	CCTGTAACCCCAGTGTGTCC	3002-2983	E11		956 (509)
TRPC5 (NM_012471.2)	F	TGAGAACGAGAACCTGGAG	1153-1171	E2		489
	R	TACTCGGCCTTGAACTCATTC	1641-1621	E3		
TRPC6 (NM_004621.5)	F	GCCTTGCTACGGCTACTACC	569-588	E1	P1	1222 (1039, 874)
	R	TCCCAGAAAAATGGTGAAGG	1790-1771	E5		
	F	AGTTTTAAGACACTGTTCTGG	2445-2465	E8	P2	551
	R	TTCTGATATTGTCTTGGAGG	2995-2976	E11		
	F	TACGATGGTCATTGTTTTGC	2564-2583	E8	P3	476
	R	TCTGGGCCTGCAGTACATATC	3039-3019	E12		
	R	TTTCCTTCAGTTCCCCTTCT	3084-3064	E13		
TRPC7 (NM_020389.1)	F	ATCTTCGTGGCCTCCTTCAC	1441-1460	E5		
	R	AACGCTGGGTTGTATTTGGC	1838-1819	E6		398

Note: F: forward, R: reverse. The predicted size for splicing variants is given in brackets.

Supplementary table 2. **Sequences of TRPC siRNAs**

TRPC1 siRNA†	T1siRNA	GCCCGGAAUUCUCGUGAAU[dT][dT]
	T1siRNA_as	AUUCACGAGAAUUCCGGGC[dT][dT]
TRPC4 siRNA	T4siRNA	UGCUCCCUAUAGAGACCGC[dT][dT]
	T4siRNA_as	GCGGUCUCUAUAGGGAGCA[dT][dT]
TRPC5 siRNA†	T5siRNA	GCAACCUUGGGCUGUUCAU[dT][dT]
	T5siRNA_as	AUGAACAGCCCAAGGUUGC[dT][dT]
TRPC6 siRNA	T6siRNA	GCAUGACUCGUUUAGCCAC[dT][dT]
	T6siRNA_as	GUGGCUAAACGAGUCAUGC[dT][dT]

†: Same as in the reference 2.